NAVAL POSTGRADUATE SCHOOL
Monterey, California

THESIS

PRELIMINARY INVESTIGATION OF THE
ENVIRONMENTAL SENSITIVITY OF ACOUSTIC SIGNAL
TRANSMISSION IN THE WAVENUMBER DOMAIN WITH
RESPECT TO SOURCE DEPTH DETERMINATION

by

Billy Barton Stamey, Jr.

December 1982

Thesis Advisors: A. B. Coppens
                      C. R. Dunlap

T208803

SECURITY CLASSIFICATION OF THIS PAGE (When Data Entered)

REPORT DOCUMENTATION PAGE		READ INSTRUCTIONS BEFORE COMPLETING FORM
1. REPORT NUMBER	2. GOVT ACCESSION NO.	3. RECIPIENT'S CATALOG NUMBER
4. TITLE (and Subtitle) Preliminary Investigation of the Environmental Sensitivity of Acoustic Signal Transmission in the Wavenumber Domain with Respect to Source Depth Determination		5. TYPE OF REPORT & PERIOD COVERED Master's Thesis December 1982
		6. PERFORMING ORG. REPORT NUMBER
7. AUTHOR(s) Billy Barton Stamey, Jr.		8. CONTRACT OR GRANT NUMBER(s)
9. PERFORMING ORGANIZATION NAME AND ADDRESS Naval Postgraduate School Monterey , California 93940		10. PROGRAM ELEMENT. PROJECT. TASK AREA & WORK UNIT NUMBERS N6846282WR200099
11. CONTROLLING OFFICE NAME AND ADDRESS Naval Postgraduate School Monterey, California 93940		12. REPORT DATE December 1982
		13. NUMBER OF PAGES 119
14. MONITORING AGENCY NAME & ADDRESS(if different from Controlling Office) Commanding Officer Naval Ocean Research and Development Activity Code 520 NSTL Station, MS 39529		15. SECURITY CLASS. (of this report) Unclassified
		15a. DECLASSIFICATION/DOWNGRADING SCHEDULE

16. DISTRIBUTION STATEMENT (of this Report)

Approved for public release; distribution unlimited

17. DISTRIBUTION STATEMENT (of the abstract entered in Block 20, if different from Report)

18. SUPPLEMENTARY NOTES

19. KEY WORDS (Continue on reverse side if necessary and identify by block number)

Wavenumber; Acoustic Signal; Sound Transmission; Source Depth; Depth Determination; Environmental Acoustic; Parabolic Equation; Acoustic Models; Lloyd's Mirror; Surface Interference

20. ABSTRACT (Continue on reverse side if necessary and identify by block number)

The Wavenumber Technique (WT) is a relatively new method of underwater sound transmission analysis. One aspect, source depth determination, is studied to evaluate its validity and test environmental and acoustic sensitivity. The horizontal wavenumber spectrum is analyzed to determine null spacings in wavenumber space, which indicates source depth by the Lloyd's Mirror interference effect. Comparison of this theory with cases of an isospeed sound profile, fully absorbing bottom, and flat totally-reflecting

DD FORM 1473 EDITION OF 1 NOV 68 IS OBSOLETE
1 JAN 73
S/N 0102-014-6601

Unclassified

20.
surface shows excellent agreement for several parametric variations. Cases with realistic sound speed profiles and partially absorbing bottoms generally agree with theory, but a distinct bias is observed. Source depth determination curves, which relate scaled wavenumber spectral intensity null spacing to the source depth, are presented for comparison with theory and sensitivity analysis. An example is given for suggested application of source depth determination.

Preliminary
Investigation
of the Environmental Sensitivity of
Acoustic Signal Transmission in the Wavenumber Domain
with Respect to Source Depth Determination

by

Billy Barton Stamey, Jr.
Lieutenant, United States Navy
B.S., College of Charleston, 1976

Submitted in partial fulfillment of the
requirements for the degree of

MASTER OF SCIENCE IN METEOROLOGY AND OCEANOGRAPHY

from the

NAVAL POSTGRADUATE SCHOOL
December 1982

ABSTRACT

The Wavenumber Technique (WT) is a relatively new method of underwater sound transmission analysis. One aspect, source depth determination, is studied to evaluate its validity and test environmental and acoustic sensitivity. The horizontal wavenumber spectrum is analyzed to determine null spacings in wavenumber space, which indicates source depth by the Lloyd's Mirror interference effect. Comparison of this theory with cases of an isospeed sound profile, fully absorbing bottom, and flat totally-reflecting surface shows excellent agreement for several parametric variations. Cases with realistic sound speed profiles and partially absorbing bottoms generally agree with theory, but a distinct bias is observed. Source depth determination curves, which relate the scaled wavenumber spectral intensity null spacing to the source depth, are presented for comparison with theory and sensitivity analysis. An example is given for suggested application of source depth determination.

TABLE OF CONTENTS

6

LIST OF TABLES

8

LIST OF FIGURES

TABLE OF SYMBOLS

α = attenuation coefficient

β = scaled wavenumber

ψ = envelope function

λ_o = reference wavelength

ω = angular frequency

ρ = density

θ = beam elevation (depression) angle

δ = central-difference operator

π = 3.141593

∇ = Laplacian operator

∂ = partial derivative operator

Σ = summation operator

$\int$ = integral operator

$\sqrt{}$ = square root operator

$<<$ = much less than

C = sound speed

C_o = minimum sound speed

C_p = normal mode phase speed

E = Lloyd's Mirror pressure field in range space

f = frequency

F = Lloyd's Mirror pressure field in wavenumber space

G = Green's function

H_o = Hankel function

I_s = spectral intensity

Im_T = imaginary pressure transform

J_o = zero order Bessel function

K = total wavenumber

k_r = horizontal wavenumber component

k_{ro} = initial spectrum wavenumber

k_z = vertical wavenumber component

Δk = wavenumber increment

K_{max} = maximum wavenumber

M = complex modified index of refraction

n = index of refraction

$\tilde{n}$ = modified index of refraction

n_b = water/bottom interface index of refraction

N = spectrum index

p = acoustic pressure

R = range

ΔR = range increment

Re_T = real pressure transform

u = wave speed

Z = water column depth

$\tilde{Z}$ = modified water column depth

ΔZ = depth increment

13

Z_R = receiver depth

Z_S = source depth

Z_{max} = maximum depth in transform

ACKNOWLEDGEMENT

I. INTRODUCTION

The Wavenumber Technique (WT) is a new method for the solution of several problems related to the analysis of underwater sound transmission (Lauer,1979). Its basis is the analysis of acoustic propagation in the wavenumber domain, which has been described by DiNapoli (1971) and was an intermediate step in the computation of transmission loss versus range in the Fast Field Program (FFP). DiNapoli (1977) later used the wavenumber domain to study the impedance of the ocean-bottom interface. Lauer (1979) first introduced the WT and its applications to passive localization and tracking and multipath decomposition. He developed a range prediction curve based upon peak wavenumbers in the transform spectrum for successive range increments from an entire pressure range field.

These investigations presented highly beneficial and promising results from the wavenumber depiction, which indicates that additional research is appropriate. One particular aspect of the WT - determination of source depth - will be investigated here in order to evaluate its validity in comparison with the Lloyd's Mirror effect. Its relationships to oceanic and acoustic variations will also be examined.

The wavenumber technique as first described by Lauer (1979) was based upon input from the FFP, but it has been adapted for use with the Parabolic Equation (PE) method of propagation loss determination. The PE-based WT is currently being investigated by Lauer and others at the Naval Ocean Research and Development Activity (NORDA) and was the model used in this research at the Naval Postgraduate School (NPS). Descriptions of the PE and WT will be presented to display their sensitivities to variations of several model parameters. Also, expected relationships of the WT to other current propagation prediction models will be discussed to consider how results might vary based upon different inputs. Particular attention will be given to algorithm differences, degrees of approximation, and treatment of the ocean bottom.

The PE-based WT will then be exercised for several parameter variations to evaluate qualitatively the consistency of the technique. This study will also demonstrate the response of the PE-based WT to geometric and actual oceanic conditions. Prediction curves for source depth determination based upon these variations will be presented and discussed.

II.   WAVENUMBER TECHNIQUE

A.   GENERAL DESCRIPTION

The WT is a natural alternative for signal depiction because it provides information on the directions of energy arrivals. It allows reasonably direct physical interpretation of ocean acoustic processes and their relationships to environmental conditions (Lauer, 1979). Lauer further states that the wavenumber spectrum plot is clearer and more informative than typical curves of propagation loss versus range.   The wavenumber K relates the angular frequency and the sound speed by

$$K = \frac{\omega}{C} = \frac{2\pi f}{C} ,$$

and it has horizontal and vertical components

$$K = k_r + k_z .$$

The reference wavenumber is determined by the sound speed minimum

$$K_o = \frac{\omega}{C_o} .$$

The WT will first be described without reference to any particular propagation model to present the general nature of the algorithm. Fig. 1 is the flow diagram for the WT. The left and right sides of this flow diagram correspond to the intensity and wavenumber axes, respectively, of the spectrum plot that will result from the WT. This figure and the following discussion were developed from Lauer (1979 and 1982a) and augmented by several telephone conversations with R. Lauer, T. Lawrence, and R. Evans of NORDA between July and December, 1982.

The WT calculates spectral intensity from the real and imaginary parts of the acoustic pressure

$$ p = \psi(R,Z) \, e^{-i\omega t} . $$

The complex psi versus range field at a specified depth is the propagation model product which determines the pressure. The complex pressure field can be modified for effects such as attenuation, depending upon whether idealized or realistic conditions are being investigated. A Fast Fourier Transform (FFT) is then applied to yield transformed complex pressure. The spectral intensity is determined at each

Figure 1.   Wavenumber Technique Flow Diagram.

21

wavenumber increment from the transformed complex pressure
field by

$$I_s \propto Re_T{}^2 + Im_T{}^2 .$$

This intensity field is scaled arbitrarily for satisfactory
display of the relative maxima and minima to define the
intensity nulls.

Additional output parameters from the PE which are
required for the WT include the range step, the number of
range points, frequency, minimum sound speed and field
depth. These are the selected variables noted in figure 1.
The range step is selected to provide sufficient resolution
to determine the wavenumber null spacing on the spectrum
plots. The initial radial component of the wavenumber for
the spectrum is calculated from DiNapoli (1971) by

$$k_{ro} = K_o - \frac{2\pi}{\Delta R}$$

where

$$K_o = k_{ro} + k_{zo} .$$

22

As will be seen in section II-B, if a "scaled" wavenumber beta is used for the horizontal axis, analysis is simplified since the nulls in the spectra should be more evenly spaced (Lauer,1979). The physical meaning of beta will be described in the next section. The resulting scaled wavenumber spectra are then plotted. The wavenumber null spacing for each incremental source depth is determined from each scaled spectrum. The source depth determination curve is generated by plotting these null spacings as a function of source depth, as suggested by Lauer (1979). The null spacing of an analyzed received signal could be compared with this determination curve to infer the source depth of the signal. This application will be discussed later. The source depth determination curve will be specific for the acoustic and oceanic descriptions of the medium.

B. PHYSICAL DESCRIPTION

The preceding description was intended to provide the overall concept of the WT whereas what follows will explain the physical basis for the technique. The underlying principle of the WT as described by Lauer (1982a) is the Lloyd's Mirror effect, which gives the acoustic field by

$$p = E(R) \ e^{-i\omega t},$$

where

$$E(R) = \frac{\exp\{iK\sqrt{R^2 + (Z_R - Z_S)^2}\}}{\sqrt{R^2 + (Z_R - Z_S)^2}} - \frac{\exp\{iK\sqrt{R^2 + (Z_R + Z_S)^2}\}}{\sqrt{R^2 + (Z_R + Z_S)^2}}$$

for a point source in a semi-infinite medium of constant
sound speed with a pressure release surface.   This is the
Lloyd's Mirror field in range space, whereas the Lloyd's
Mirror field in wavenumber space, applicable to this
research, is given by Lauer (1982) as

$$F(K) = \frac{\sin(\beta Z_S)}{\beta} \exp(i\beta Z_R) ,$$

where beta is defined by

$$\beta = (K_o^2 - k_r^2)^{\frac{1}{2}} ,$$

and E(R) and F(K) are related by the Bessel transform pair

$$E(R) = \int_0^\infty 2\, F(K)\, J_o(KR)\, K\, dK$$

and

$$F(K) = \frac{1}{2} \int_0^\infty E(R)\, J_o(KR)\, R\, dR \quad .$$

24

For this research the Bessel function was approximated as a trigonometric function so that the FFT could be utilized. This is considered acceptable since the source and receiver are greatly separated, according to Lauer (1982b). Inspection of F(K) reveals that the nulls of the spectrum will be equally spaced at intervals of

$$\Delta\beta = \frac{\pi}{Z_S}$$

This equal spacing in beta is the key element of the application of the WT to source depth determination (Lauer, 1979).

Only the direct and surface-reflected waves will interact at a receiver location in a simple illustration of the Lloyd's Mirror effect with a smooth surface. This interaction will be destructive or constructive, as a result of their relative phases (Kinsler et al ,1982) and will produce nulls or peaks, respectively, in the wavenumber spectrum. Fig. 2 depicts the Lloyd's Mirror effect geometry which will be used to study test case outputs for null spacing and subsequent source depth determination. The surface-reflected (SR) wave travel distance will increase at a faster rate than the direct (D) wave distance as the source is moved

25
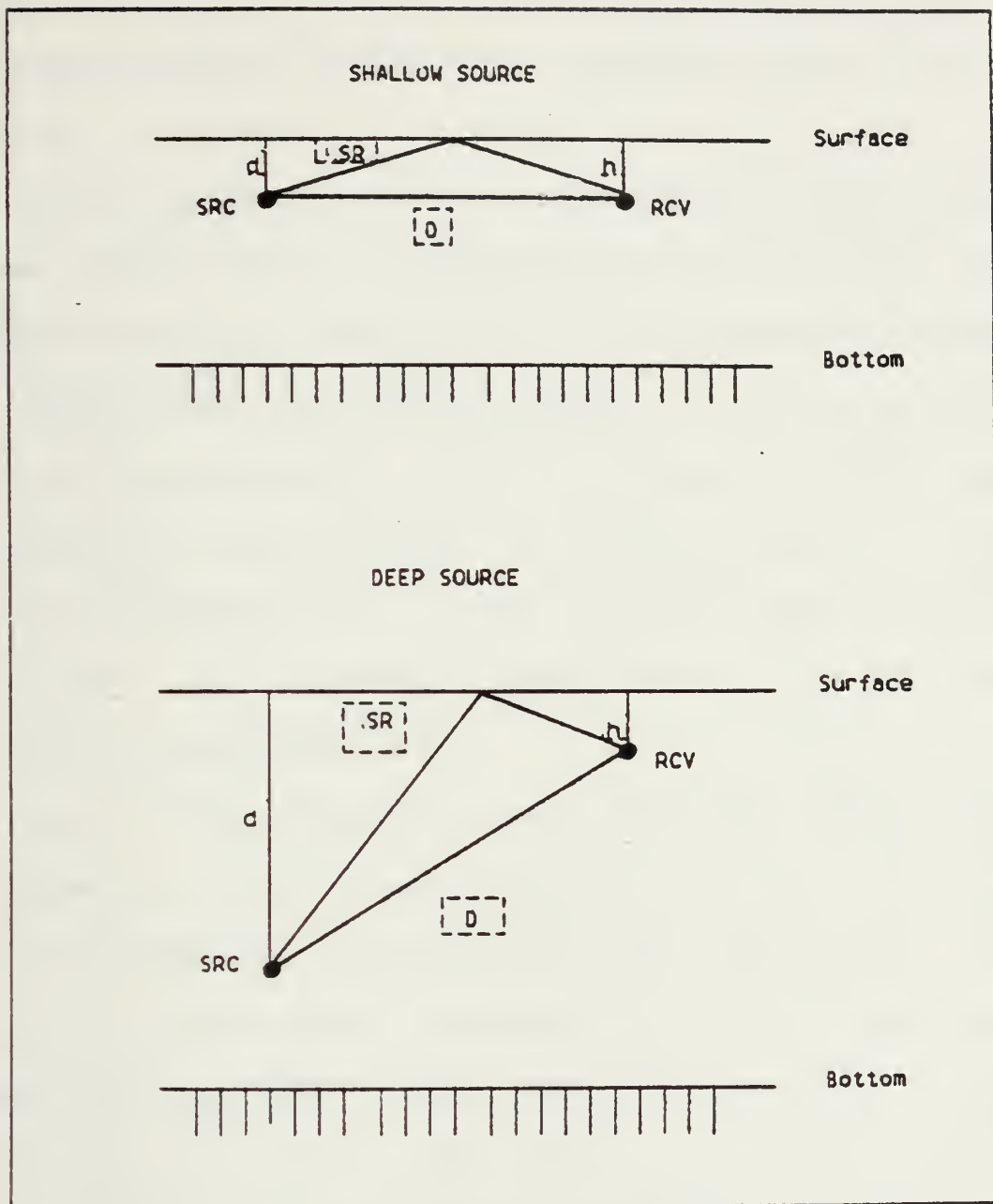
Figure 2. Lloyd's Mirror Effect Geometry.

26

deeper in the water column (d) while the receiver depth (h) is stationary. This leads to different arrival patterns and nulls at more wavenumbers. Thus the general pattern of decreased spacing in beta with increasing source depth is observed.

Bottom interacting waves will be neglected for idealized cases. This will be accomplished by the use of a fully absorbing bottom. These waves will be important, however, in shallow water or at greater ranges. A few test cases will have realistic bottoms. Various propagation models handle the bottom in different ways, so the inclusion of a bottom will be discussed later. Cases in shallow water (less than 5000 feet) or at extended ranges (greater than 100 miles) will not be considered here.

Lauer (1979) observed that the wavenumber spectrum shows a series of modulating envelopes which enclose spikes that are the eigenvalues associated with the normal modes. Comparison of the wavenumber spectrum with typical transmission loss curves reveals that the wavenumber depiction is more coherently structured. This leads to a better physical understanding of signal transmission because of the relationship between horizontal wavenumber and ray theory. He gives this as

$$k_r = \frac{\omega}{C} \cos\theta = \frac{2\pi f}{C} \cos\theta .$$

The horizontal wavenumber decreases as theta increases. Thus the wavenumber axis of the spectrum plot will include wavenumbers associated with smaller elevation (or depression) angles in increasing order of wavenumber (Lauer,1979). It is then expected, for the case of a neglected bottom, that spectrum amplitude peaks could be observed that would correspond to the direct and surface reflected waves.

C. WAVENUMBER TECHNIQUE APPLICATION

Lauer (1979) recommends a receiver that is a single omnidirectional hydrophone and a source-generated continuous wave (CW) received signal for source depth determination. He further states that in actual use the single hydrophone could be replaced by an array to improve the signal-to-noise ratio and to obtain bearing and bearing rate information.

An example of a possible application of the WT, source depth determination, is presented in Fig. 3. A propagation model could be run for a series of incremental source depths to yield the null spacing relationship, as was shown in Fig. 1. That curve would be specific to the properties of the ocean and values for parameters such as frequency and receiver depth. A received signal as shown on the right side of Fig. 3 could then be analyzed. Its null spacing could be
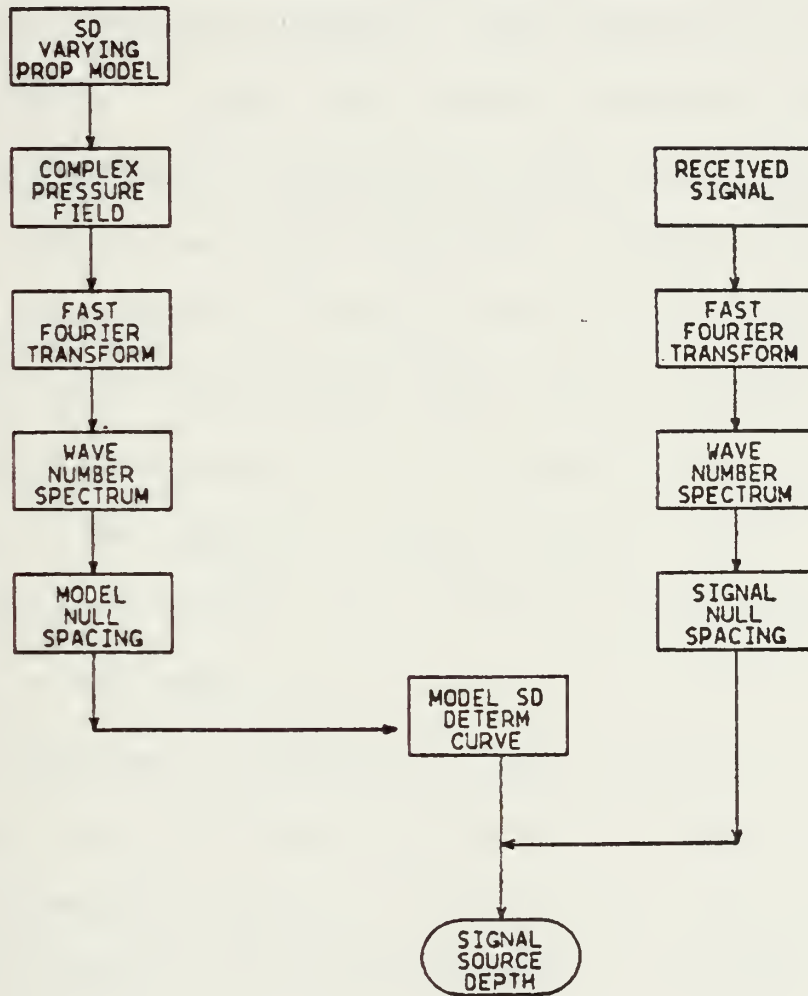
Figure 3. WT Application for Source Depth Determination.

compared to the model-produced curve to infer the depth of the source.

D. TECHNIQUE LIMITATIONS

The success of the WT is related directly to the accuracy of the predicted pressure field produced by the propagation model. There are several possible differences between propagation models which might affect the pressure field. Some of the more significant include approximations of the wave equation, bottom effects, initial source functions and input limitations. These will be compared for several models to determine relevant restrictions. The pressure field will also respond to changes in the ocean. A series of different scenarios will be run to provide an initial estimate of the sensitivities to some of these factors.

Any additional limitations will be related to computer processing time and storage requirements. These factors will not be addressed directly in this research because the processing following the propagation model is minimal. There is also no requirement to store the complex pressure fields or their transforms once the null spacing has been determined. Thus the WT computer utilization is directly proportional to the time and storage required for the propagation models.

III. PROPAGATION MODELS

A. INTRODUCTION

Modeling the propagation of sound in the ocean is complicated by the variability of the ocean, the great range of frequencies of interest, and the many applications of sound propagation (DiNapoli and Deavenport,1979). It is not surprising that no single model is presently capable of addressing all of these variations; there are many semi-restrictive methods. In general all models consider the sound speed to be a function of the spatial coordinates and independent of time (DiNapoli and Deavenport,1979). Only the frequency, water column geometry and oceanic description will affect propagation.

All models, regardless of application, can be divided into two classes: range independent or range dependent. Range independent models assume that the ocean is cylindrically symmetrical, the speed of sound is a function only of depth and all boundaries are planar perpendicular to the depth axis (DiNapoli and Deavenport,1979). Range dependent models can provide better approximations of real conditions

by allowing the sound speed to be a function of two or three spatial variables. They also do not require planar boundaries perpendicular to the depth axis, thus cylindrically symmetric bottom topography can be included (DiNapoli and Deavenport,1979). A range-dependent model, the split-step Fast Fourier Transform PE (SSFFT) was the numerical model used in this research to generate the pressure fields for the wavenumber analyses. This PE will be qualitatively compared to two other range-dependent algorithms, a range-modified Normal Mode (NM) model and a Finite Difference (FD) model. It will also be compared to a range-independent method, the Fast Field Program (FFP) model. The range-dependent capability of the SSFFT was not used in this research since this was an initial investigation. Its comparison with both range dependent and independent models may, however, indicate possible model effects on the WT which could be studied later.

In general all models attempt to solve the acoustic wave equation. This equation is valid for sound propagation in fluid media with specified boundary conditions (Urick,1975,p.114). It becomes the reduced elliptic Helmholtz equation in spatial coordinates under the assumption of harmonic time dependence.

32

B.   PARABOLIC EQUATION

   1.   Introduction

      The PE algorithm used in this research was developed
by Brock (1978).   The basic feature of this PE is the
replacement of the reduced elliptic Helmholtz equation by a
parabolic partial differential equation that utilizes the
Tappert-Hardin split-step Fourier algorithm (SSFFT) for the
numerical integration (Brock,1978).   The original computer
code as described by Brock has been modified to incorporate
the source and attenuation descriptions of Tatro (1977) and
to include an ocean bottom by Stieglitz et al (1979).   This
is the version of the PE that is currently available at NPS
and was the code (PEMODEL) used for this research.   (It must
be emphasized that some difficulty was encountered in trying
to   ascertain the   correct description   of   the NPS   version
because of inadequate and   erroneous comment card documenta-
tion in the   source code and incomplete   manuscript descrip-
tions.)

      This section   will discuss the SSFFT,   the original
Brock algorithm, modifications to that code,   and subsequent
evaluations of the   SSFFT.   Particular   attention will   be
given to those aspects which are expected to affect the WT.

2. Parabolic Approximation

The parabolic approximation to the wave equation was first introduced by Leontovich and Fock (1946) as a solution for the propagation of electromagnetic waves along the surface of the earth. Its first introduction to underwater acoustics was by Hardin and Tappert (1973) who used the split-step technique in conjunction with the FFT to solve this particular approximation to the wave equation. The result was the SSFFT. Tappert (1977) related the use of the parabolic approximation to sound channel propagation in a waveguide that is thin vertically and elongated horizontally to the range of the first convergence zone or farther.

Long-range propagation, with which the SSFFT is basically concerned, will usually be for low frequencies because volume absorption increases strongly with frequency (Tappert, 1977). The maximum elevation (and depression) angles of propagation for long range transmission must be small to satisfy the PE (Tappert, 1977). The derivation of the SSFFT will be discussed later in a simplified version as presented by Brock (1978).

It appears that the SSFFT is intended for use in situations where bottom interaction and surface scattering

34

would be negligible. Thus the use of the SSFFT to examine
the Lloyd's Mirror effect in the real world may be inappro-
priate if the ocean surface is sufficiently rough; addi-
tional errors may occur in situations where bottom effects
are significant.

   3. Brock Algorithm

      a. Description

         The SSFFT is valid for acoustic pressure in a
medium of constant density with a monofrequency source and
cylindrical symmetry about the depth axis (Brock,1978). The
acoustic pressure can be written as

$$p(R,Z) = \psi(R,Z) \, H_o{}^1(K_o R) \, ,$$

where the zero-order Hankel function of the first kind
relates the acoustic pressure to an outward propagating
cylindrical wave envelope function (Brock,1978). This is
valid because of the assumption that at low frequencies all
significant energy will propagate approximately horizontally
away from the source (Tappert,1977). The asymptotic form of
the Hankel function is

$$H_o{}^1(K_o R) \approx \{2/\pi K_o R\}^{\frac{1}{2}} \exp\{i(K_o R - \pi/4)\} \quad , \quad K_o R \gg 1 \, ,$$

if the receiver is many wavelengths from the source. This leads to (Brock,1978)

$$\psi_{RR} + 2iK_o\psi_R + \psi_{ZZ} + K_o^2\{n^2(R,Z) - 1\}\psi = 0 .$$

The additional assumption of neglecting the far field effects,

$$|\psi_{RR}| << |2iK_o\psi_R| \quad ,$$

is the "parabolic" approximation for radial transmission (Brock,1978). The result is the Leontovich-Fock (1946) PE

$$\psi_R = i(A+B)\psi ,$$

where

$$A = \frac{-1}{2K_o} \frac{\partial^2}{\partial z^2}$$

and

$$B = \frac{Ko^2}{2} (n^2 - 1)$$

which is the form used by Brock (1978).

b. Implementation

Brock (1978) used the SSFFT to solve the PE because it has several significant advantages which outweigh its disadvantages. Advantages include exponential accuracy in depth, second-order accuracy in range, energy conservation, unconditional stability and computational efficiency. Disadvantages are a uniform mesh and periodic boundary conditions to satisfy the FFT, and filtering of the sound speed profile by smoothing discontinuities to avoid spurious high angular-frequency components (Brock,1978). Additionally the algorithm assumes a flat pressure-release surface, a vanishing field at the maximum depth and a pseudo-radiation condition at the water-bottom interface by smoothly attenuating the field (Brock,1978).

A numerical algorithm of

$$\psi_R = i(A+B)\psi \quad ,$$

$$\psi(R+\Delta R,Z) = e^{i\Delta R(B+A)} \psi(R,Z) \;,$$

leads to

$$\psi(R+\Delta R,Z) = e^{i\Delta RB} \; FFT^{-1}\{ \; e^{i\Delta RA} \; FFT \; (\psi(R,Z)) \; \}$$

37

or

$$\psi(R+\Delta R, Z) = e^{i\Delta R K_o (n^2-1)/2} \, FFT^{-1}\{e^{i\Delta R K^2/2K_o} FFT(\psi(R,Z))\}$$

to facilitate the computations since a spatial FFT and its inverse are required to transform between depth and wavenumber (Brock,1978). This procedure is implemented by two alternating steps, the first of which considers propagation in a homogeneous medium to account for diffraction and the second to account for refraction (Brock,1978). In his development Brock gives an alternate calculation of the envelope function stemming from

$$\psi(R+\Delta R, Z) = e^{i\Delta R A/2} \, e^{i\Delta R B} \, e^{i\Delta R A/2} \, \psi(R,Z) \, ,$$

This differs slightly from the previous expression containing the FFT and inverse FFT. Thus it is not currently known which relationship is used by Brock; this could be resolved later by a detailed examination of the computer code. In any event as McDaniel (1975a) has shown, either approach would be of sufficient accuracy with appropriate selection of ΔR and ΔZ.

The SSFFT appears to be quite satisfactory numerically, but it has to simplify the actual oceanic variability to allow realistic computation. It apparently will handle source and receiver depths and horizontal separation distances well as noted by its degrees of accuracy in depth and range. The smoothing of the sound speed gradients and bottom effects will have to be considered.

The intent of this description has been to provide a base from which comparisons can be made with other numerical solutions and modifications to this algorithm. The effect of the source model on the WT can be evaluated by these comparisons. The primary elements of the WT are the real and imaginary parts of the complex pressure amplitude. Thus the algorithmic differences with respect to computation of the pressure field will be the primary basis for the comparison of effects on the WT.

McDaniel (1975a) compared the basic Tappert and Hardin SSFFT, which is used by Brock, to normal mode theory. She found that errors arise in phase and group speeds, although one mode can be propagated with the correct amplitude and group and phase speeds. McDaniel describes three sources of error: (1) approximating the wave equation by the

SSFFT as noted above, (2) limiting the range steps and permissible sound speed gradients, and (3) truncating the field at a finite depth. The result of the SSFFT will be a shift in the modal interference at long ranges if many modes are propagating (McDaniel,1975a). The error due to range step limitations is third order in the range step increment (McDaniel,1975a), thus a small range step is required to minimize this error. The third error is related to inclusion of a highly absorbing bottom which causes preferential attenuation of higher-order modes; the dominant contribution will thus result from the lower modes (McDaniel,1975a).

Brock et al (1977) have described a procedure to improve this condition. It maps the index of refraction and depth such that the phase speeds and turning points of the normal modes are preserved. This involves construction of a "pseudoproblem" such that the parabolic phase speeds will be equal to the elliptic phase speeds of the corresponding modes in the original problem (Brock et al ,1977). This is given as

$$(n,z) \rightarrow (\tilde{n},\tilde{z}) = \{(2n-1)^{\frac{1}{2}} , zn^{\frac{1}{2}}\} \ .$$

It is found to greatly improve the SSFFT agreement with the elliptic solution. This correction technique has one basic constraint, which is that isospeed regions are not allowed in the sound speed profile because of poor eigenfunction mapping (Brock et al, 1977).

   4.   Subsequent Modifications

      a.   Introduction

         There have been two significant modifications since the original algorithm was published by Brock (1978). These are source function and volume attenuation alterations (Tatro,1977) and the incorporation of a bottom and variable range step (Stieglitz et al ,1979). The Tatro modification was developed in 1977 but was added to the Brock algorithm after 1978. Discussion of these two aspects will complete the description of the PE algorithm installed at NPS and utilized in this study.

      b.   Tatro Modifications

         The Gaussian source originally utilized by Brock (1978) was considered to be inefficient in terms of program size limitation and an upper frequency limit which is relatively low (Tatro,1977). A new source function was developed. This was intended to solve the problem of large

vertical wavenumbers from a Gaussian source that were previously eliminated with range (Tatro,1977) and led to an incorrect depiction of the field.

This source is basically a low pass filter in the vertical wavenumber domain which is centered at the source depth (Tatro,1977). The initial vertical wavenumber field will thus be a constant up to a prescribed value and zero for higher wavenumbers. The use of the filter is claimed to yield improvement over the Gaussian source by minimizing the aliasing which might occur upon transforming to the depth domain (Tatro,1977). The benefits derived from the use of this new source are reduced computation time and storage and the availability of higher frequencies (Tatro,1977).

He also modified the Brock algorithm by introducing volume absorption as calculated from the equation of Thorp (1967). The decision can be made whether or not to include volume absorption.

c. Stieglitz et al Modifications

Brock (1978) had considered the PE most useful for long range propagation at low frequencies and small grazing angles. The bottom was modeled as fully absorbing so

that the field would vanish at the maximum depth of the transform. This depth was obtained by extending the water column depth by one-fourth to obtain the transform depth. The index of refraction in this region was

$$n^2 = n_b{}^2 + iae^{-\{(Z-Z_{max})/b\}^2}$$

where a and b are empirical constants. The energy in the bottom was attenuated such that any additional modes which resulted from transform truncation were minimized. This empirical expression was selected to coincide with a comparable normal mode solution. This rather crude model of the bottom appeared to be acceptable for situations wherein the bottom had a relatively small effect.

Stieglitz et al (1979) considered it necessary to attempt to develop a more realistic ocean bottom since acoustic propagation was being utilized in more varied and extreme situations where bottom interaction was important. They developed two additional options for handling the bottom: (1) a partially absorbing bottom with specification of reflective loss versus grazing angle of the equivalent ray and (2) the direct insertion of sediment sound speed and

43

attenuation profiles.   The algorithm derives the sediment profiles from the grazing angle loss values in the first option. The supplied profiles are used directly in the second option (Stieglitz et al ,1979).   A new complex modified index of refraction

$$M(R,Z) = \{n^2(R,Z) - 1\} + i2b(Z)/K_o$$

is computed if the bottom attenuation is to be calculated.

One additional change, the calculation of the range step, has also been added by Stieglitz et al (1979). It consists of an initial search of the vertical wavenumber domain for the maximum pressure component. This is then followed by a search for the first component which is 50 dB below the maximum component.   The wavenumber of this component

$$k_z = K_o \sin\theta_{50}$$

is stated to require a range step of

$$\Delta R = \lambda_o/(1 - \cos\theta_{50}),$$

where

$$\lambda_o = 2\pi/K_o .$$

The range step was fixed in the current research for the
benefit of the spatial transform in the WT, thus the above
description was not utilized. It has been included to com-
plete the description of the computer code which apparently
comprises the NPS model, PEMODEL.

5. SSFFT Evaluations

The SSFFT has been investigated on several occasions
to examine specific items which might be modified to yield
better agreement with actual propagation. Most of these
studies deal with the algorithmic description by Tappert and
Hardin (1973). Examination of these studies will note fur-
ther possible limitations on accuracy in the SSFFT which can
be extended to the WT.

Fitzgerald (1975) examined the accuracy of the SSFFT
as a function of range and frequency. It was shown that the
SSFFT demonstrated greater accuracy at longer ranges, the
lower the frequency. The SSFFT was considered a good
approximation in the examples given for 100 HZ and 10 HZ to

about 111 and 15000 km, respectively (Fitzgerald, 1975).
The current study will examine transmission at 50 and 100 HZ
at ranges to 100 nautical miles. These ranges will exceed
the limits of Fitzgerald in some cases.

McDaniel (1975b) investigated splitting the total
field into transmitted and reflected fields in deriving the
SSFFT. It was necessary to neglect the reflected field for
the matrix associated with the Tappert-Hardin SSFFT, since
the two fields did not decouple where the wavenumber was
independent of range (McDaniel, 1975b). Thus an exact
expression could not be determined for the transmitted field
without the reflected field. (The reflected field is neg-
lected in the current research since it uses the SSFFT.)
This will lead to phase speed and group speed errors as
McDaniel (1975a) pointed out earlier, as discussed in Sec-
tion III-B-4. These errors were minimized by Brock et al
(1977) by a mapping technique for both the index of refrac-
tion and the depth. Even so, the implication of this possi-
ble error on the WT is that the interference patterns may
not be exact, which will lead to inexact or biased wavenum-
ber nulls. McDaniel (1975b) proposed another matrix which
achieved the desired decoupling and thus allowed expressions

46

for the transmitted and reflected fields. This alternative was not investigated in this initial research. It may be a way to resolve non-exact results and could be studied later to isolate quantitatively the biases related to various input parameters for the WT.

Palmer (1976) related possible inaccuracies in the SSFFT to approximations involving relatively small terms in the exponential approximations for the operators A and B and also to the use of a single reference wavenumber. These approximations will not be investigated specifically in this research but they may be related to potential disagreement between the SSFFT and the theoretical Lloyd's Mirror effect. The association of errors due to a single wavenumber can be recognized from the wavenumber spectra, which will be presented later in section IV-A. They will show not only an energy concentration at the reference wavenumber but significant energy distributed, as well, over a range of values. Palmer (1976) emphasized that the physical properties of the ocean must be considered before terms can be neglected, such as the spreading of energy over several wavenumbers.

DeSanto (1977) studied the relationship between the acoustic pressure and the envelope function (called velocity

potential by DeSanto), which is directly relevant to the current research where pressure is calculated from the modeled envelope function. DeSanto arrives at

$$\psi(R,Z) = A_0 R^{1-2a} \int_0^\infty P(t,Z)\, Q(R,t,Z)\, \exp\,(iK_0/Zt)(R^2+t^2)\, t^{a-3/2} dt \;,$$

where Q satisfies

$$Q_{RR} + 2\{(1-a)/R + (iK_0 R)/t\}Q_R + Q_{ZZ} + 2iK_0 Q_t + 2Q_Z \frac{\partial}{\partial z}\{\ln(p(t,Z))\} =$$

$$K_0^2 \{K_2(t,Z) - K_2(R,Z)\}Q$$

and

$$K_2(R,Z) = K(R,Z) - K_1(Z)$$

The PE for the envelope function is obtained if this function is evaluated by stationary phase; thus, it appears that a more accurate result could be obtained by better evaluation of the integral. DeSanto et al (1978) developed a correction for the SSFFT, known as the Corrected Parabolic

48

Approximation (CPA), that handled phase inaccuracies better than the SSFFT. Further study might address the response of the WT to the CPA with respect to improved phase accuracy as a function of range.

6. Environmental Sensitivity of the PE

This final section in the analysis of the PE will consider the expected environmental sensitivity of the PE, and, by extension, the WT. The important relationship of the PE to the WT is the input of the complex pressure amplitude and ultimately the resultant wavenumber distribution. As discussed earlier in Section II-B, the wavenumber could be associated to the source angle and, by extension, to the ray type or family (Lauer, 1979). Consequently, oceanic parameters which modify the transmission of certain rays can be related to the resulting wavenumber distribution.

The sound speed profile will favor certain ray paths at different depths in the water column. There should be a corresponding shift in ray paths and hence wavenumbers as the source and receiver depth geometry is changed. The direct and surface-reflected rays will travel at different speeds depending upon the gradients along the profile and thus lead to different spatial interference patterns. This

can lead to wavenumber shifts and changes in the null spacing. Profiles used in the current study will include real examples and isospeed cases.

Another important aspect is the transmission geometry. Generally the model will be run at considerable range and in relatively deep water, which will be consistent with the applicability of the PE. A series of source depths with a single fixed receiver depth will be run to generate the wavenumber null spacing values that will formulate a determination curve for each case of geometrical variation. The distribution of these resulting curves can be examined to evaluate the effects of transmission geometry on the WT.

Two frequencies will be examined in a similar manner. This would be one of the most important parameters to investigate in future studies since it would have a direct bearing on operational applications. It is expected that there will be differences in the resulting wavenumber spectra depending on the input frequency. The relationship between frequency and transmission geometry will also be studied since these are the easiest parameters to vary during an experiment and will lead to the most complete analysis of model variability.

The surface will be assumed to be planar and pressure-release so that there will be complete specular reflection. The minimum source depth used will be that at which a definable interference pattern can be observed for the specified frequency. The slope approaches zero near the surface on the source depth determination curves. This result may indicate that the WT in its current form is probably not applicable for sufficiently shallow sources.

The final important area of variability will be the bottom boundary conditions. There are several options now available in the PEMODEL. The fully absorbing and partially absorbing bottoms will be considered. A fully absorbing bottom will be used in most cases to simplify the interference pattern by eliminating any rays which interact with the bottom. Thus the basic interference pattern may be evaluated. Various bottoms can then be tested to study the effect of the bottom on the WT. Differing bottom loss curves will be compared in a few cases to demonstrate qualitatively that the bottom does have an effect. The third bottom option of a realistic sediment sound speed could also be investigated once the general effect of the bottom has been determined. It would not offer any additional significant

results at this point beyond those realized from the fully- and partially- absorbing bottoms.

All input parameters are related and thus the examination of any one particular factor must be considered with respect to the full range of variation of the other factors. The number of combinations of parameters would be very large for a model such as the PEMODEL. Thus this research can only begin to explore general relationships. Additional research is necessary to delineate specific parameter impacts on the WT.

C. FAST FIELD PROGRAM

1. General Description

The Fast Field Program (FFP) was selected as the first model to compare to the PEMODEL since it was the origin of the WT and the initial testing of the WT by Lauer (1979) was performed with the FFP. The description of the FFP which follows is summarized from DiNapoli (1971).

The basic result of the FFP is direct numerical integration by the application of the FFT to field theory to compute propagation predictions in a minimum computation time. The pressure can be represented in the form

$$p(R,Z) = \sqrt{\rho} \int_{-\infty}^{\infty} G(Z_R, Z_S; K) \ H_o{}^1(KR) \ K \ dK \ ,$$

where G, the Green's function, must satisfy

$$\frac{d^2 G}{dz^2} + \{K^2(Z) - k_r{}^2\} G = -\delta(Z - Z_S)$$

and the associated boundary conditions. The field equation can then be written as

$$p(Z, R_m) = \sqrt{\rho} \; \Delta K (2/\pi i)^{\frac{1}{2}} \; e^{iK_o R_m} \; /R_m{}^{\frac{1}{2}} \; E_m{}^{\frac{1}{2}} \; e^{imR_o \Delta K} \quad ,$$

where

$$E_m = G(Z, Z_S; K_m) \; K_m{}^{\frac{1}{2}} \; e^{imR_o \Delta K} \quad .$$

In this form, p can be obtained through use of the FFT at each range increment. Given p as a function of range, the WT could be applied as usual. DiNapoli compared an example from the FFP with the normal mode program of Bartberger and Ackler (1973) and found excellent agreement between the locations of the peaks and the real parts of the eigenvalues. The only significant difference is that the FFP includes more higher order modes but does not include the

53

first four modes. DiNapoli states that the FFP offers a
significant reduction in computation time yet still provides
reasonable results as compared to normal node theory. This
is accomplished by expressing the sound velocity profile as
one or more exponential functions of depth. These exponen-
tial functions allow the use of recurrence relations to
quickly calculate the input to the FFT.

The FFP offers two options for the modeling of the
bottom; a two-layered fluid bottom with specified sound
speeds and a semi-infinite bottom of one sound speed. The
propagation effect from the first would be eventual return
of rays once reflected from the second bottom interface. The
semi-infinite bottom would not allow any return of sediment
rays.

2. Comparison of FFP and PE

The FFP is a range independent model and the PE is
range dependent. The environment was considered constant
over the range in the current research, and thus the two
models can be compared. The FFP uses the sound speed profile
as an exponential function which is a different approach
from the linear segmentation of the PE. The number of expo-
nential functions could be sufficient to model an actual

profile approximately as well as the PE. The PE bottom modeling does not appear to offer any significant advantage in theory over the FFP, which allows for a semi-infinite or layered bottom. It is likely from a theoretical standpoint that the PE and FFP inputs to the WT could be similar enough to allow comparison. The wavenumber spectrum shows a series of peaks which result from the nearby singularities of the Green's function. These can be expressed as the normal modes. The utility of the WT stems from the spacing of the nulls between the envelopes which contain these peaks.

D.   NORMAL MODE THEORY

   1.   General Description

        The fundamental importance of the normal mode solution, and the reason that is it used to check the validity of other models, is that it is an exact solution to the wave equation (Kinsler et al ,1982,p. 430). The following description continues from Kinsler et al (1982,pp. 430-432).

        The solution for a point source is given by

$$(\nabla^2 - \partial^2/C^2 \partial t^2)\ p = \frac{1}{4\pi}\ \delta(\vec{R}-\vec{R}_o)\ e^{j\omega t}\ ,$$

where

$$\vec{R}_o = (0, Z_S)\ .$$

55

Analysis yields

$$p = e^{j\omega t} (-j\pi) \sum_n Z_n(Z_S) Z_n(Z) H_o^1(K_n R)$$

and Zn must satisfy

$$\frac{d^2 Z_n}{dz^2} + \{\omega^2/C^2(Z) - K_n^2\} Z_n = 0 \ ,$$

where Kn is constant and appropriate boundary conditions. This solution is for trapped modes and does not include those which are evanescent. Normal mode theory can be linked to the WT by the spatial representation of the wave-number

$$K(Z) = \frac{\omega}{C(Z)} \ .$$

The rays in the deep sound channel which have the same local direction of propagation correspond to the normal modes by the relationship

$$\cos\theta = \frac{K_1}{K(Z)} \ ,$$

56

which extends to the normal mode phase speed

$$C_p = \frac{\omega}{K_l} \, ,$$

where l designates the lth mode.

Normal mode theory lends itself to many applications in underwater acoustics and it may be formulated for both range dependent and independent situations. A dependent form which is appropriate for comparison with the SSFFT was developed by Kanabis (1975). He developed a normal-mode model which allows large changes in the sound speed profile, depth, and bottom composition with range. The range domain is segmented into regions within each of which sound speed and bottom composition are functions of depth but not range. The normal mode solutions for each region are matched at the interfaces.

2. Comparison of NM and PE

It would be expected that the WT would respond similarly to these two models. This is based upon this example of a normal mode program and supported by the previously discussed evaluation studies involving PE and NM. The NM solutions are generally applicable to long range propagation

at low frequencies, which is quite similar to the PE. The NM can be identified closely with the WT in a physical sense, because of the interference effects in the NM that result from several multiple reflections (Officer, 1958,p. 117). Officer further states that the number of reflections will increase and the time intervals between the incidence of successive reflections will decrease as the range increases. This might be comparable to depth variations which will be shown for the WT. The NM yields exact solutions for modeling with planar boundaries. Thus the results of a WT based on NM would be limited only by approximations which were intrinsic to the WT. A comparison of PE- and NM-based WT data should aid in evaluating the impact of the particular PE algorithm.

E. FINITE DIFFERENCE METHODS

1. General Descriptions

One final group of methods which has evolved recently are the finite difference methods of solution for the parabolic equations (Lee and Papadakis, 1979). They seek a more general solution which will be appropriate in shallow water or where bottom interaction will be important. They further state that the FD and ODE methods will be

superior to SSFFT because an artificial bottom is not required for the benefit of the FFT. Explicit and implicit finite difference schemes are considered as well as an ordinary differential equation. The explicit finite difference (EFD) scheme is

$$u_m^{n+1} = e^{K \frac{\partial}{\partial R}} u_m^n \quad ,$$

where u_m^n represents $\psi(Rn, Zm)$, Rn is the nth range point, and Zm is the mth depth point. The implicit finite difference (IFD) method from Lee and Botseas (1982) is

$$e^{-\frac{1}{2}K\frac{\partial}{\partial R}} u_m^{n+1} = e^{\frac{1}{2}K\partial/\partial R} u_m^n \quad .$$

The FD scheme is consistent, stable and convergent in the solution of the PE (Lee and Papadakis, 1979).

The ODE method is

$$\frac{d}{dR} u_m = a_m u_m + \frac{b_m}{(\Delta Z)^2} (u_{m+1} - 2u_m + u_{m-1}) \quad ,$$

where a and b are related by

$$u_R = a(K_o, R, Z)u + b(K_o, R, Z)u_{ZZ} \quad .$$

59

This technique is stable, consistent and convergent also which supports its use. One additional aspect of the ODE approach is the calculation of a variable range step.

2. Comparison of FD and ODE with PE

One result of the FD and ODE methods is greater flexibility in arbitrary bottom and surface boundary conditions than that available with the SSFFT. Lee and Papadakis (1979) state that while the FD and ODE methods are both superior to the SSFFT, the best appears to be the ODE, followed by the EFD, which is limited by step size. Thus the FD and ODE methods appear to be significant improvements over the SSFFT. This result should extend to a WT based upon FD or ODE input.

More recently Lee et al (1981) have re-examined the IFD and found it to be as equally efficient as the ODE. The general advantage of the IFD over the SSFFT is that the problem is solved within the water column since the bottom effects can be modeled by straight line segments. This is similar to the ODE, but the IFD does not require the amount of storage necessary for the current ODE (Lee et al, 1981). McDaniel and Lee (1982) have extended the IFD to the treatment of vertical density discontinuities. They found that

while without this more realistic treatment of the water-bottom interface the IFD approximates the SSFFT and differs significantly from normal mode, the IFD corresponds extremely well with the normal mode calculations with the interface. In conclusion, the numerical techniques related to FD and ODE appear to be viable alternatives to the SSFFT. They will permit a more accurate representation of underwater acoustic transmission, which will be directly relatable to the WT.

IV. ANALYSIS OF WT

A. GENERAL DESCRIPTION

Twenty scenarios were selected to examine the general aspects of variations in several oceanic and geometric parameters. A set of input parameters and a sound speed profile were constant in each scenario while the source depth was varied. Five to ten source depths were used for each situation. The vertical and horizontal axes of the wavenumber spectra correspond to the spectral intensity and the scaled wavenumber beta, respectively. The intensity axis was normalized to unity for ease in plotting. The null spacing was determined for each spectrum. These null spacing values were plotted versus source depths to yield the determination curve for each scenario.

Table I lists the parametric specifications for each scenario. Basically they can be divided into isospeed or sound speed profile cases. An isospeed profile of 4890 ft/s from the surface to the bottom was selected to evaluate the transmission geometry and the general consistency of experimental results, assuming a fully-absorbing bottom. The WT

is based on the arrivals of the direct and surface-reflected rays; thus, the isospeed cases will be the easiest to compare with theory. There will be no sound speed differences as a function of depth which could modify the arrival times. Additionally, several realistic ocean profiles were studied to allow a qualitative comparison with theory and explore spatial and temporal variability. It is recognized that the theoretical Lloyd's Mirror effect applies only to isospeed profiles. Results from real profiles were compared with this theory to see if they could approximate it. The spatial and temporal scales of variability used in this research were approximately 200 miles and 20 days.

More analyses were performed with the isospeed cases since this was an initial investigation. It still remains to consider other simple cases, such as linear negative and positive gradients, surface ducts and deep sound channels. Also realistic ocean studies that would involve greater temporal and spatial variations would be beneficial. Time was limited during this research, thus efforts were divided between model validation and oceanic sensitivity. It is believed, however, that the comparisons which will be presented are sufficient for a preliminary investigation into the sensitivity of the WT.

TABLE I
Scenario Specifications

ISOSPEED PROFILE

Run Set	Rcv Depth RD:ft	Range R:nm	Freq F:Hz	Water Depth Z:ft	Number of SD Runs
I0	300	50	100	10000	7
I1	300	50	50	10000	6
I2	300	100	50	10000	6
I3	300	50	100	5000	6
I4	300	100	100	5000	5
I5	300	50	50	5000	6
I6	300	100	50	10000	6
I7	300	100	100	10000	5
I8	800	50	50	10000	5
I9	10000	50	50	10000	5
R1	300	25	100	10000	5
R2	300	50	100	10000	5
R3	300	75	100	10000	5

REALISTIC PROFILE

Run Set	Rcv Depth RD:ft	Range R:nm	Freq F:Hz	Water Depth Z:ft	Src Depth SD(number)
A0	300	100	100	9000	8
A1	1000	100	100	9000	5
A2	9000	100	100	9000	5
A3	300	100	100	9000	5
B0	300	100	100	12000	8
C0	300	100	100	9000	8
D0	300	100	100	12000	8

The complex pressure input data were not modified so that the entire wavenumber spectrum would be observed at the receiver. These effects would need to be evaluated if the WT was to be compared to received signals. The surface and bottom were assumed flat. Boundary variations would have to be considered for WT use under realistic ocean conditions. A nominal beam width of thirty degrees was used and in almost all cases the range step was 0.1 mile.

Frequencies of 50 and 100 Hz, water column depths of 5000 and 10,000 feet and ranges of 50 and 100 nautical miles were the basic comparisons for most isospeed scenarios. A receiver depth of 300 feet and a fully absorbing bottom were utilized, unless otherwise noted. Additional comparisons were performed, such as range variations to 25 and 75 miles and receiver depth variations of 800 and 10,000 feet. A range of 100 nautical miles and a frequency of 100 Hz were used for the actual cases unless otherwise noted. The bottom depths were 9000 feet for profiles A and C and 12,000 feet for profiles B and D.

The realistic profiles were obtained from the Acoustic Storm Transfer and Response Experiment (ASTREX) which was conducted by NPS in the northeast Pacific Ocean in November

and December, 1980 (Dunlap,1982). The ASTREX study was con-
ducted to evaluate the effect of oceanic response to atmos-
pheric storms on acoustic propagation. The profiles were
selected for this research to represent only spatial and
temporal variability without respect to any experiment oper-
ations. The profiles were obtained from expendable bathy-
thermographs (AXBT) which were dropped by U. S. Navy P-3
aircraft. Fig. 4 shows the relative locations and times for
these profiles. The digitized profiles were analyzed by the
University of Hawaii to remove spikes and false values.
These profiles were combined with climatological salinity
profiles at the Fleet Numerical Oceanography Center in Mon-
terey. Table II gives the descriptive data for each
profile. The bottom loss curves which were used are similar
to those found in Urick (1979) and were arbitrarily devel-
oped to indicate higher loss for profiles B and D. This is
related to bottom composition; bottom types for profiles A/C
and B/D are calcareous sand and clay, respectively
(NAVOCEANO,1978). Thus higher loss is expected for B/D.

A general feature of the spectra for almost all test
cases is a distinct U-shape with peak values at the minimum
and maximum wavenumbers. Figs. 5 through 10 show this phe-
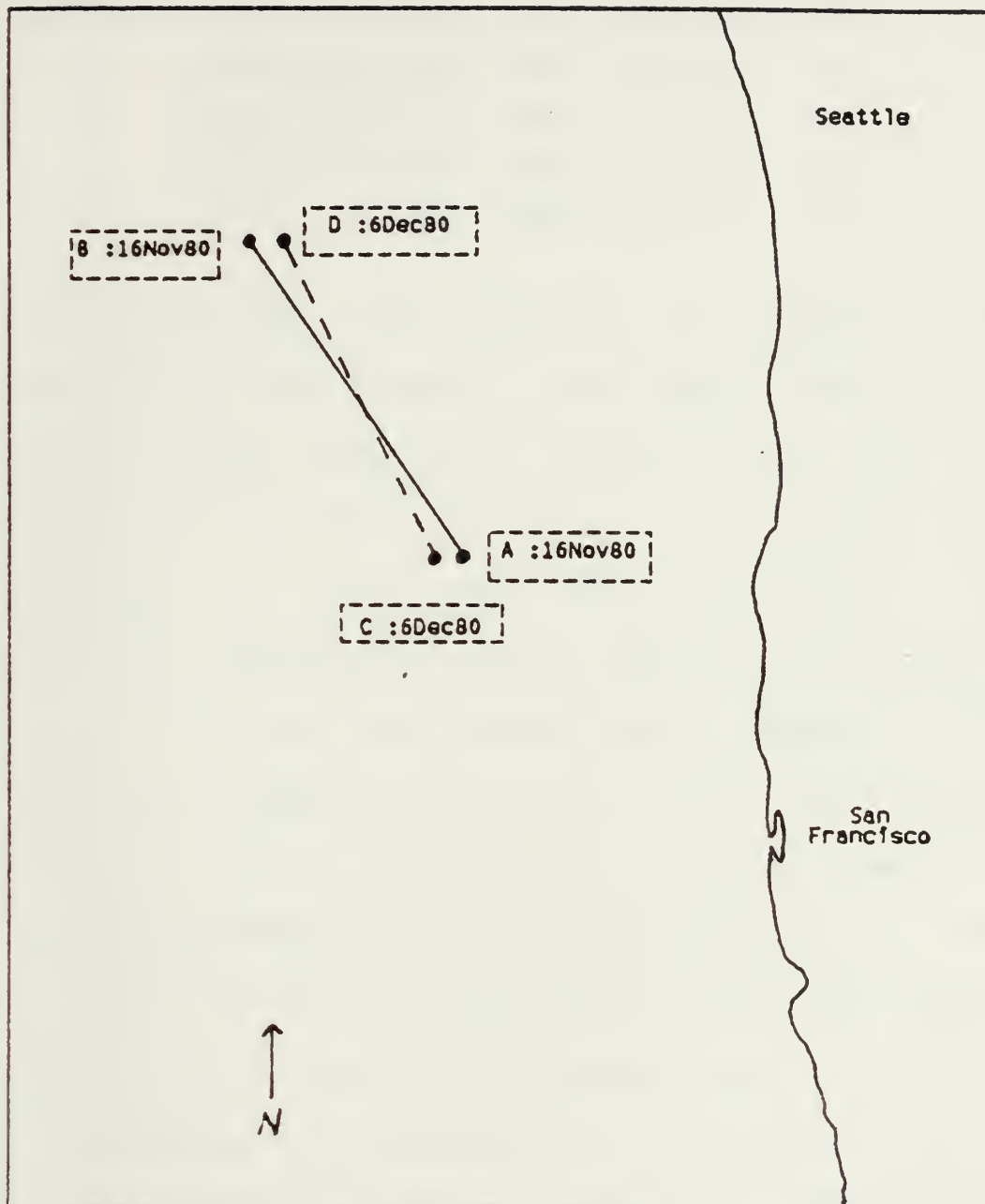
Figure 4. Space and time relationships of actual profiles.

TABLE II

Location Information for Realistic Profiles

Profile	Lat	Long	Date	Time(Z)	MLD(m)
A	41-24N	127-23W	16 NOV	1928:04	32
B	45-47N	133-05W	16 NOV	2121:25	61
C	41-23N	128-22W	6 DEC	1843:37	58
D	45-46N	133-09W	6 DEC	2033:45	79

nomenon for isospeed cases and Figs. 11 through 16 for a
realistic sound speed profile. The abbreviations on these
figures are source depth (SD), receiver depth (RD), and
water column depth (Z) in feet; range (R) in nautical miles;
and frequency (F) in Hz. This key will also apply to the
source depth determination curves which will be presented
later. The right and left intensity maxima appear to corre-
spond to beam elevation angles of 0 and 30 deg, respec-
tively, which could be considered to approximate the direct
and surface-reflected waves. A 30 deg beam angle was used;
thus, there may be a relationship with the left maximum.
This beam angle is also near the maximum angle which Tappert
(1977) considered to be appropriate. Then the left maximum
might be a result of algorithmic inaccuracy. Different beam
angles could be tested to determine if this would explain

the unexpected U-shape curve. This apparently anomalous spectral pattern might be explained by a possible transform assumption of symmetry about zero and the inclusion of negative transform values. It is also possible that the left wavenumber peak may be the result of aliasing of the high wavenumber values. DiNapoli (1971) suggested that aliasing could occur and thus he utilized only one-half of the range field. This has not been tested in the current research; however, examination of different range segments might resolve this apparent problem. A remote possibility is that the direct and surface-reflected rays each exhibit a Bessel function display. This might be depicted by a peak at the reference wavenumber for each ray with a set of interfering envelopes between the peaks. A mathematical explanation for this possibility has not yet been explored. No spikes are seen in very shallow water as depicted in Fig. 17, but also no distinct null pattern is observed, thus near surface source depths have been neglected.

These figures were also included to show a series of source depth runs and the resulting decrease in beta spacing as a function of source depth. The null spacing was manually measured for each run as the distance between two adja-

RUN I43
SD:200FT RD:300FT F:100HZ Z:5000FT R:100NM
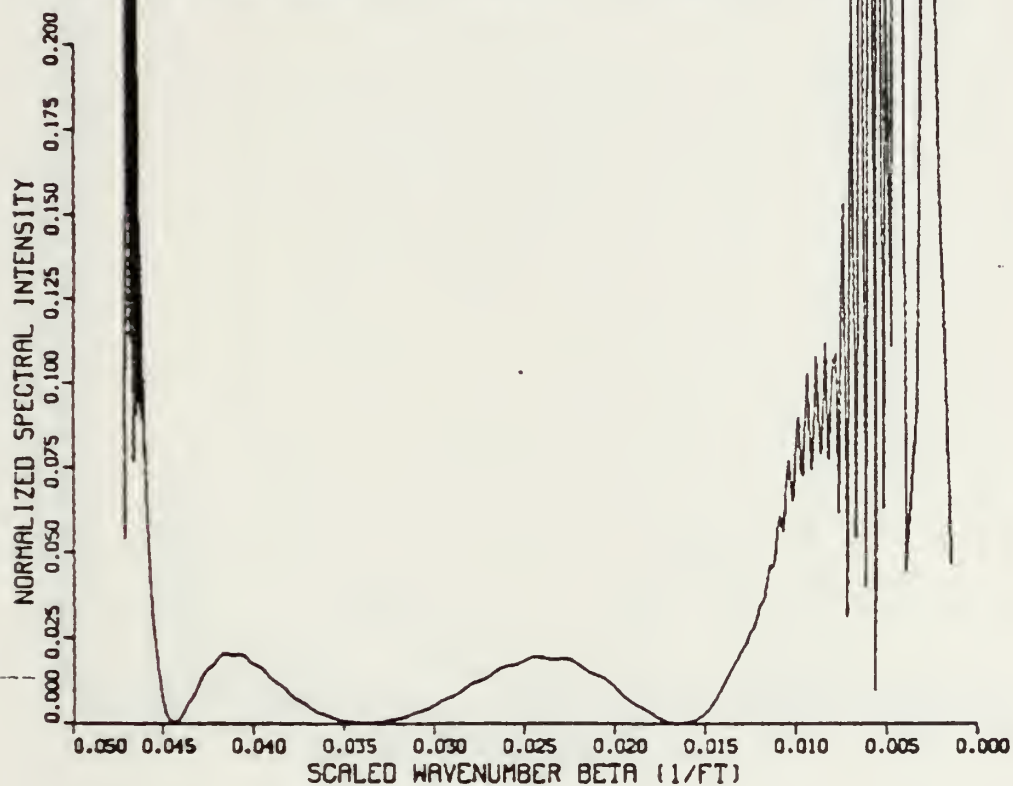
Figure 5. Isospeed Profile Wavenumber Spectrum for SD of 200 ft.
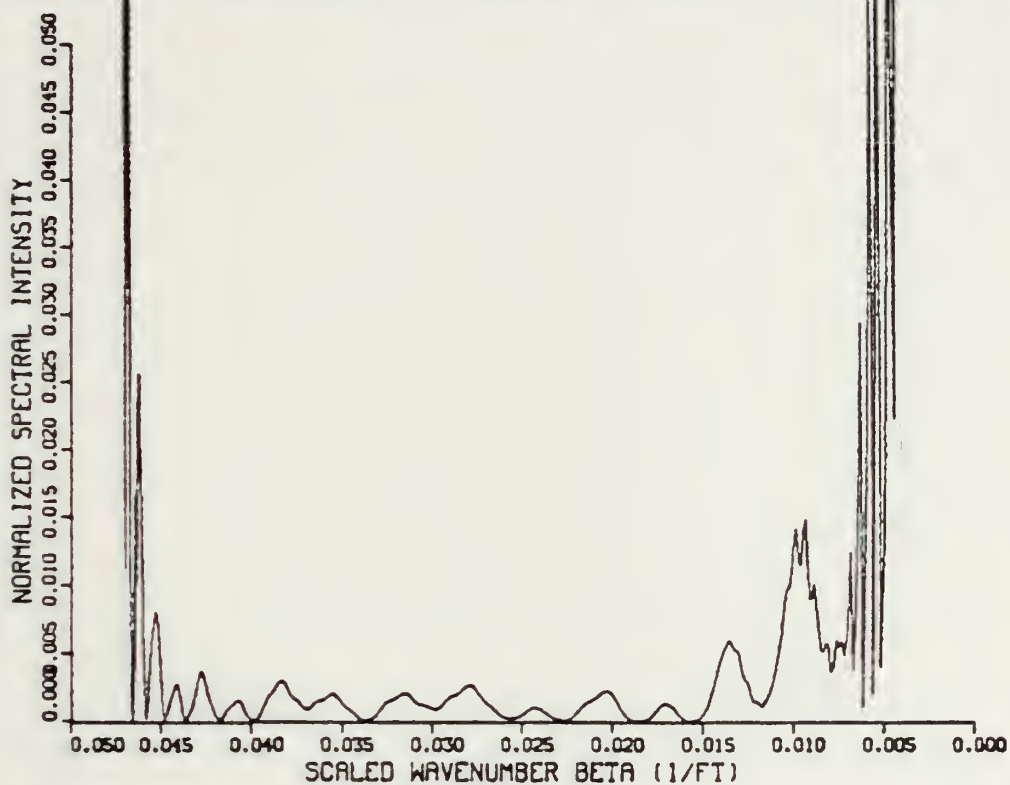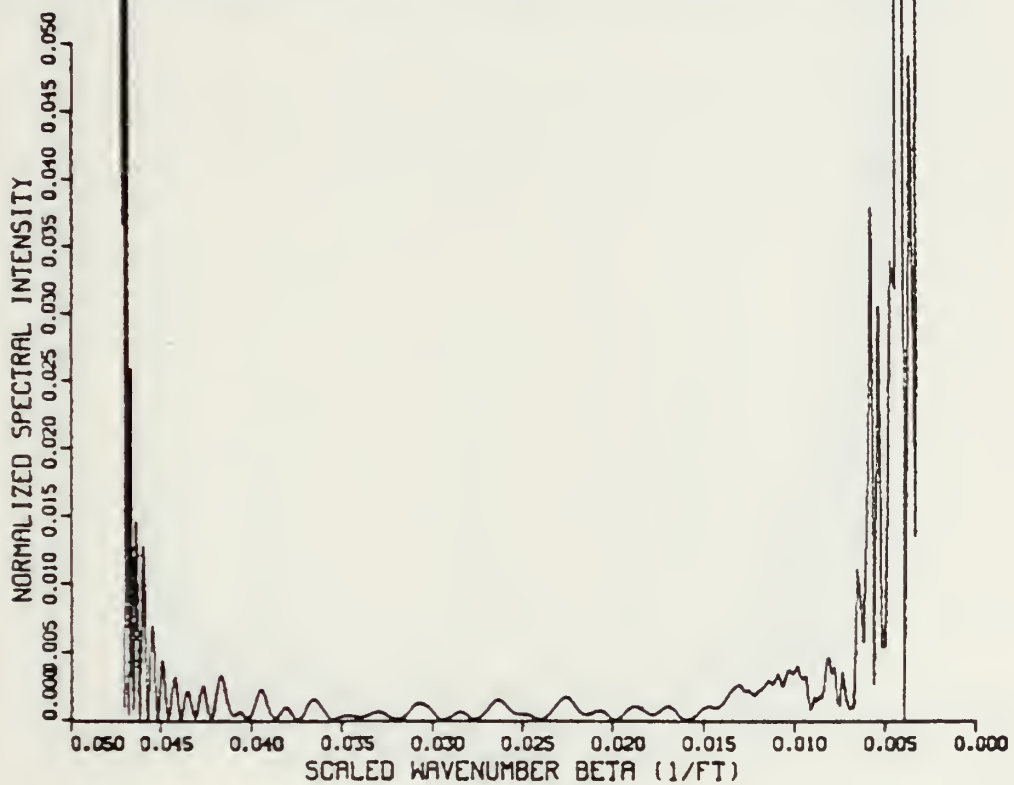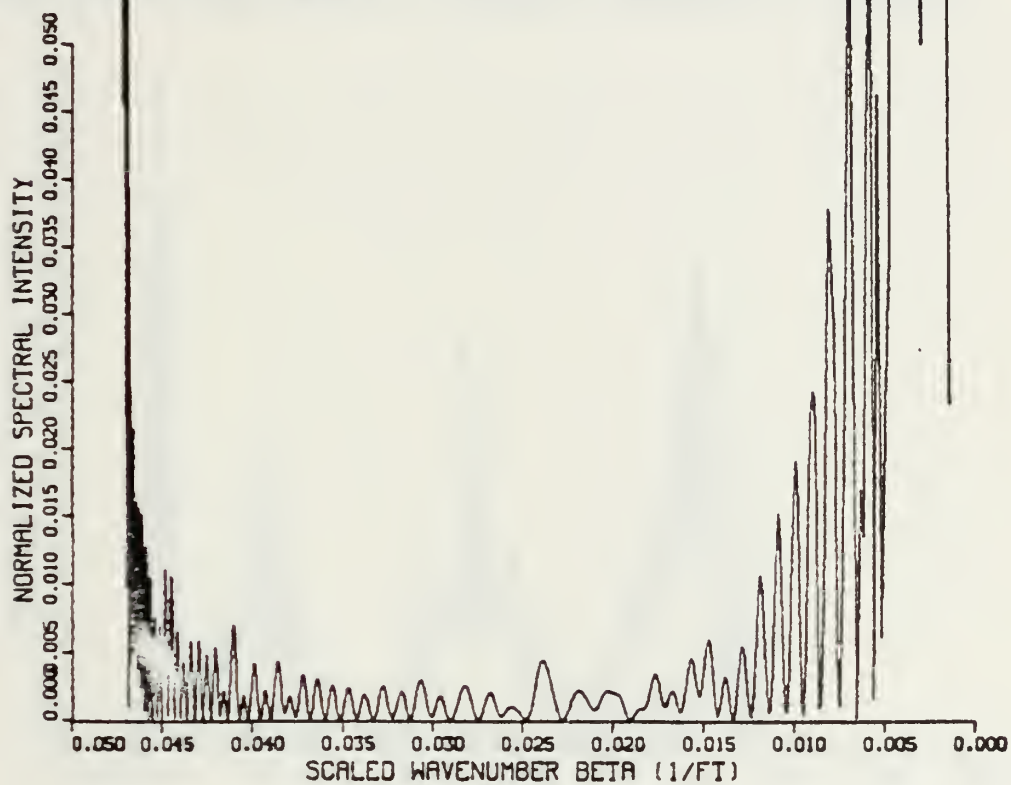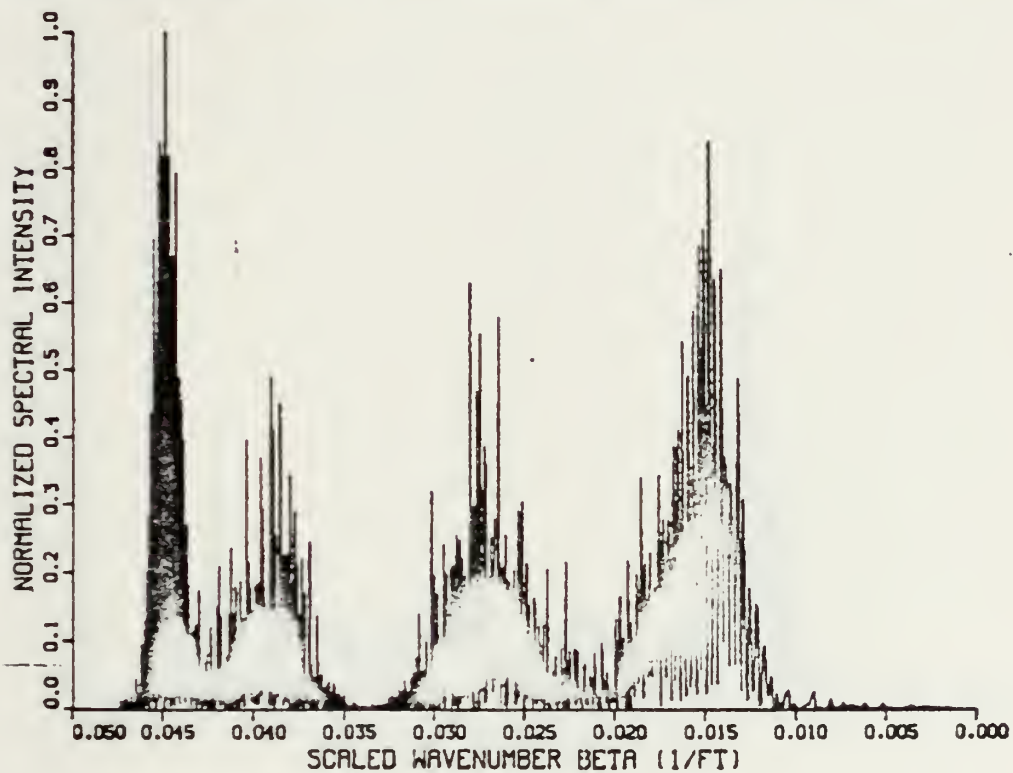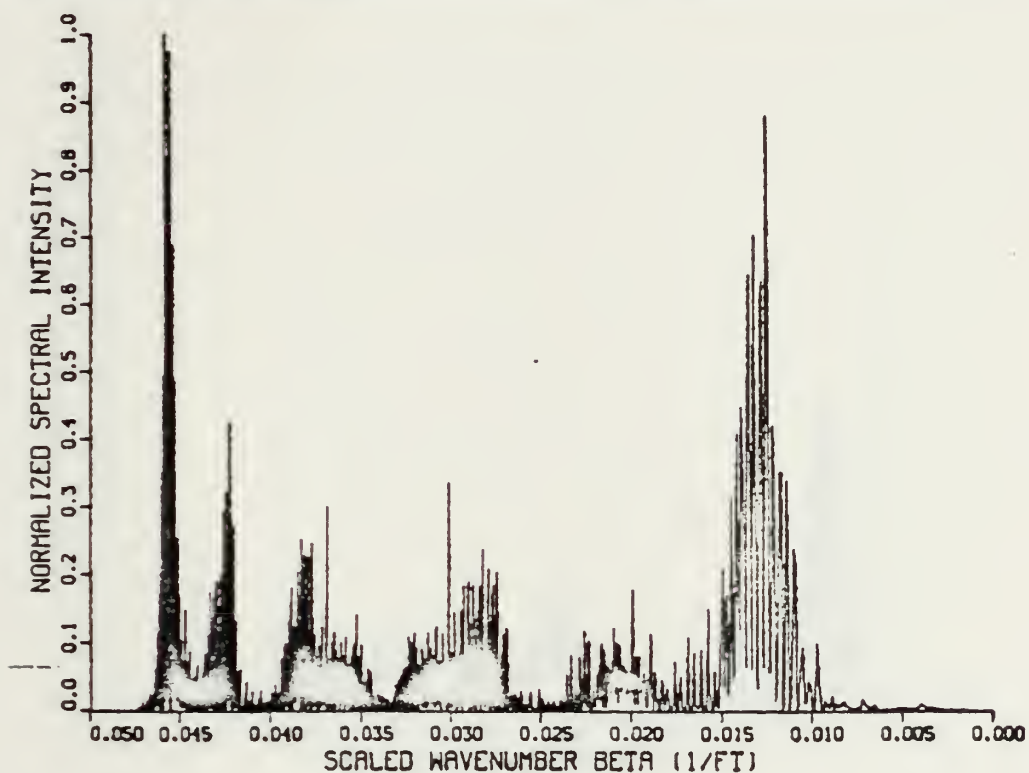
RUN 144
SD:300FT RD:300FT F:100HZ Z:5000FT R:100NM
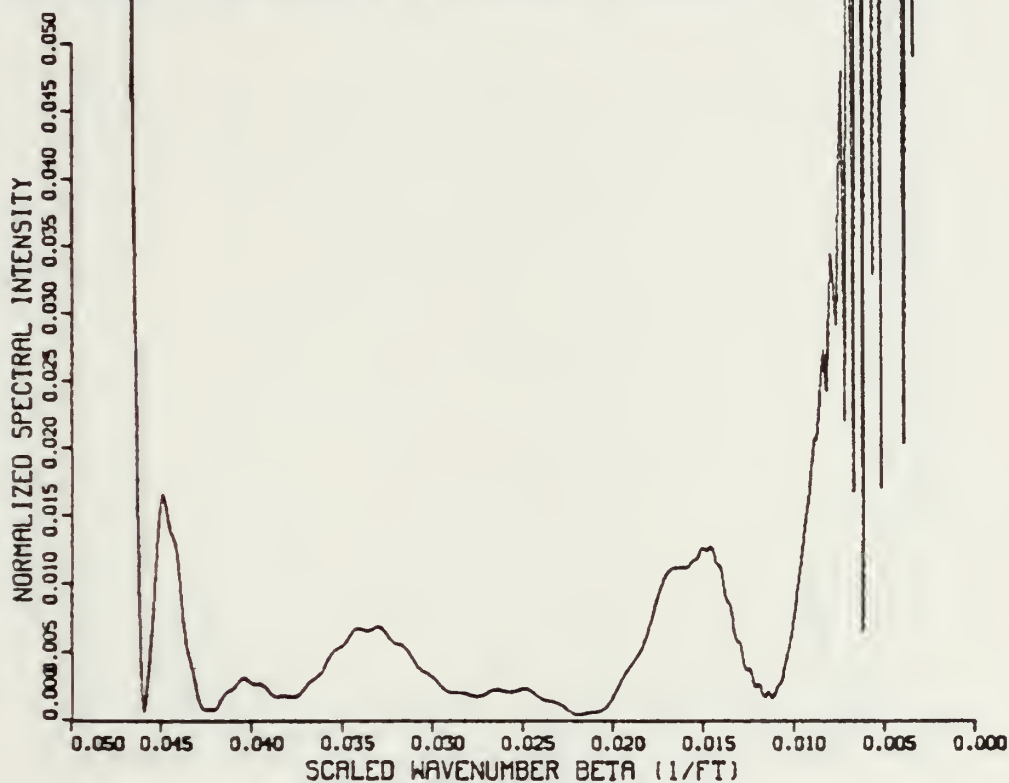
Figure 6.   Isospeed Profile Wavenumber Spectrum for SD of
300 ft.

71

RUN I45
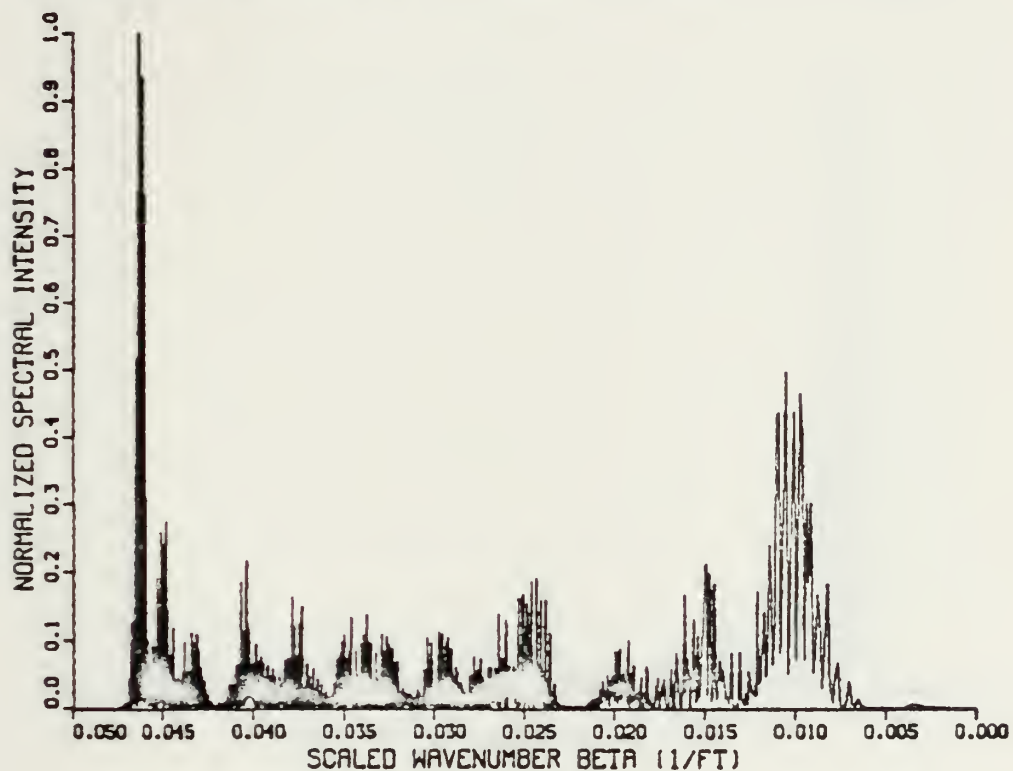SD:500FT RD:300FT F:100HZ Z:5000FT R:100NM
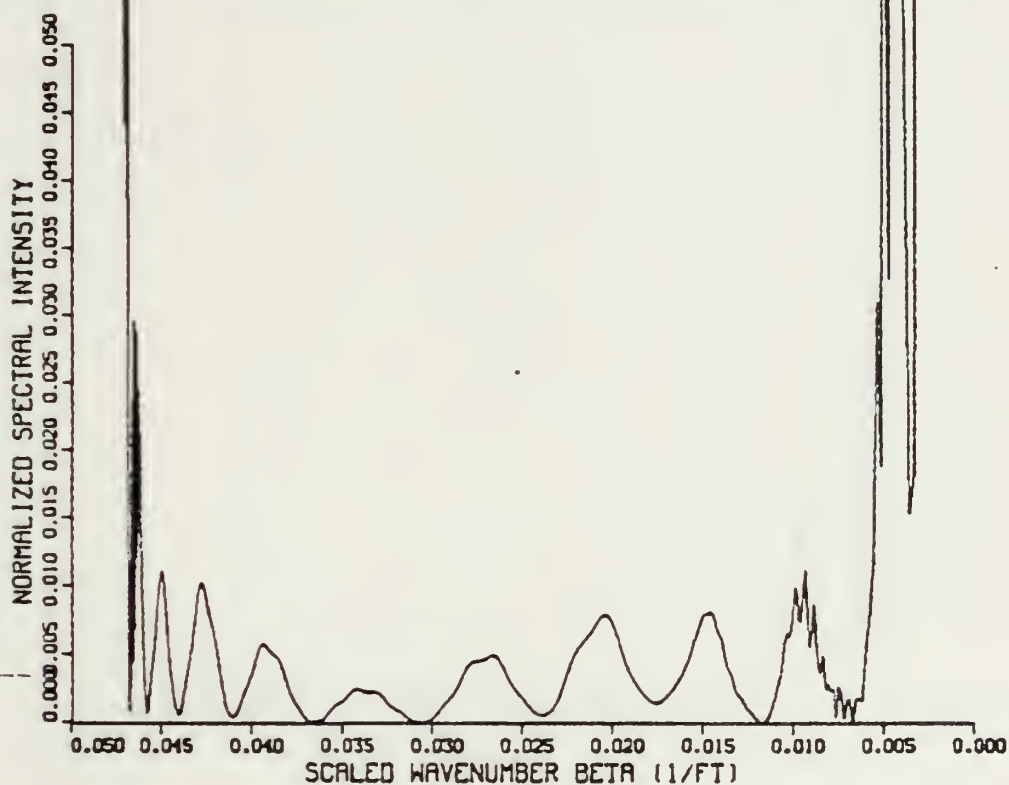
Figure 7. Isospeed Profile Wavenumber Spectrum for SD of
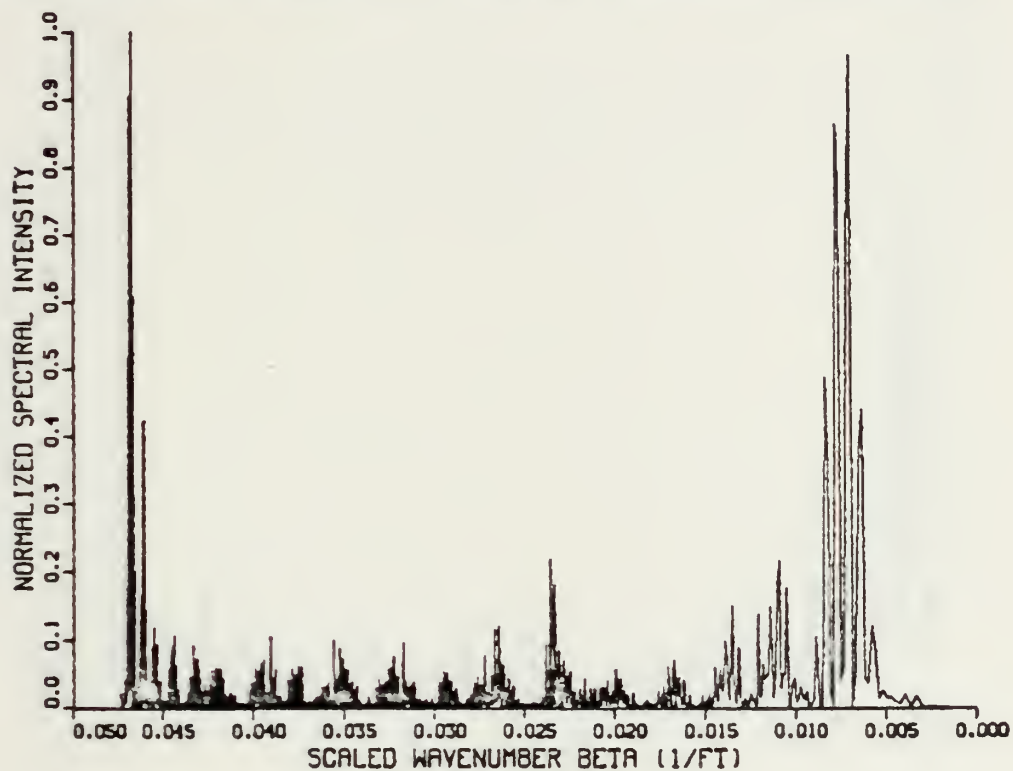500 ft.

RUN I46
SD:800FT RD:300FT F:100HZ Z:5000FT R:100NM

Figure 8.   Isospeed Profile Wavenumber Spectrum for SD of 800 ft.

RUN 147
SD:1500FT RD:300FT F:100HZ Z:5000FT R:100NM

Figure 9.   Isospeed Profile Wavenumber Spectrum for SD of
1500 ft.

74

RUN I48
SD:3000FT RD:300FT F:100HZ Z:5000FT R:100NM

Figure 10.   Isospeed Profile Wavenumber Spectrum for SD of
              3000 ft.

75

RUN A03
SD:200FT RD:300FT F:100HZ Z:9000FT R:100NM

Figure 11.   Realistic Profile Wavenumber Spectrum for SD of
             200 ft.

RUN A04
SD:300FT RD:300FT F:100HZ Z:9000FT R:100NM

Figure 12.   Realistic Profile Wavenumber Spectrum for SD of
             300 ft.
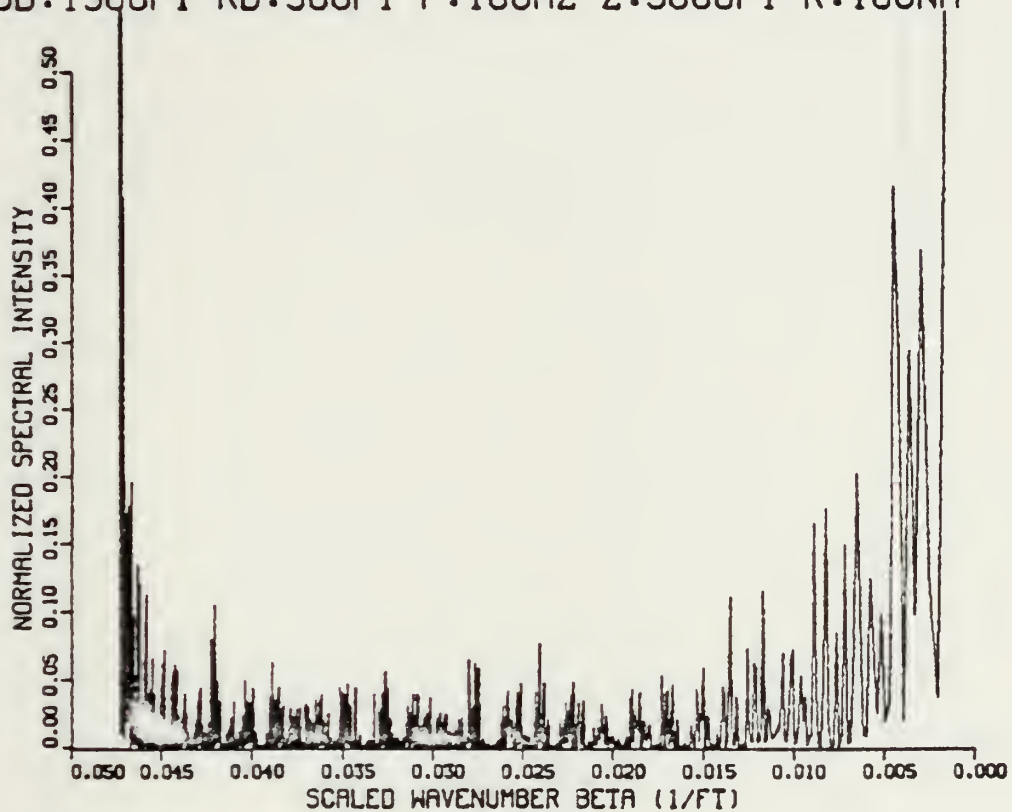
RUN A05
SD:500FT RD:300FT F:100HZ Z:9000FT R:100NM

Figure 13.   Realistic Profile Wavenumber Spectrum for SD of 500 ft.
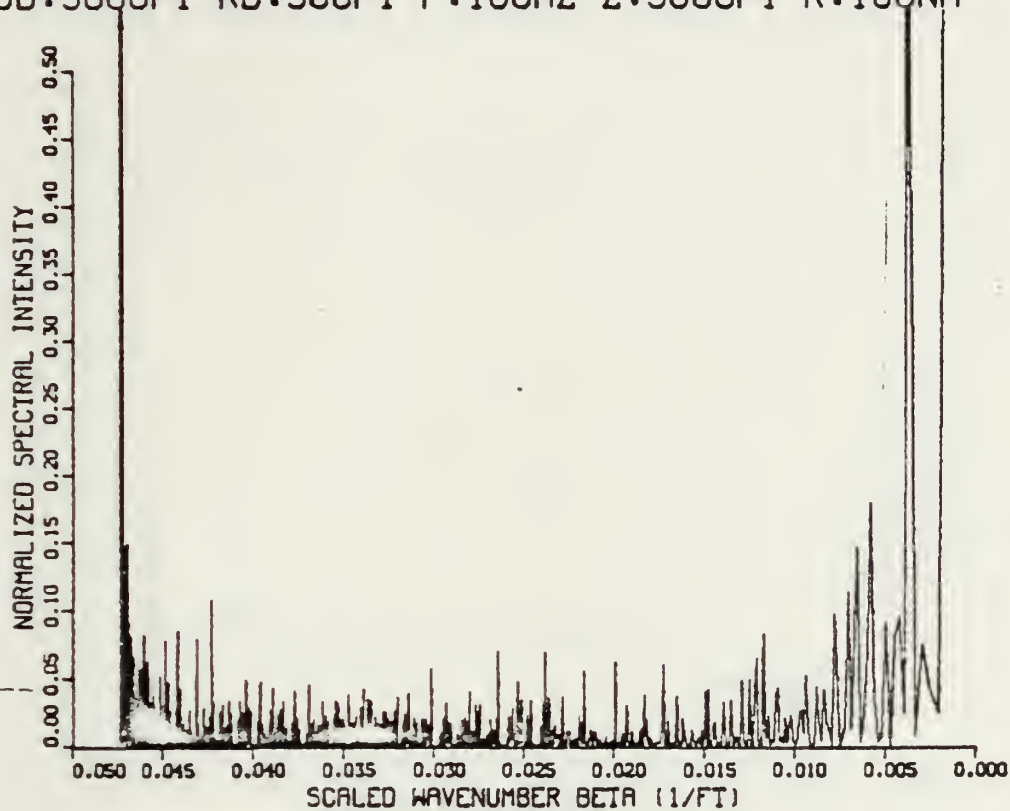
RUN A06
SD:800FT RD:300FT F:100HZ Z:9000FT R:100NM

Figure 14.   Realistic Profile Wavenumber Spectrum for SD of
800 ft.

Figure 15.   Realistic Profile Wavenumber Spectrum for SD of 1500 ft.

RUN A08
SD:3000FT RD:300FT F:100HZ Z:9000FT R:100NM

Figure 16. Realistic Profile Wavenumber Spectrum for SD of 3000 ft.

RUN I41
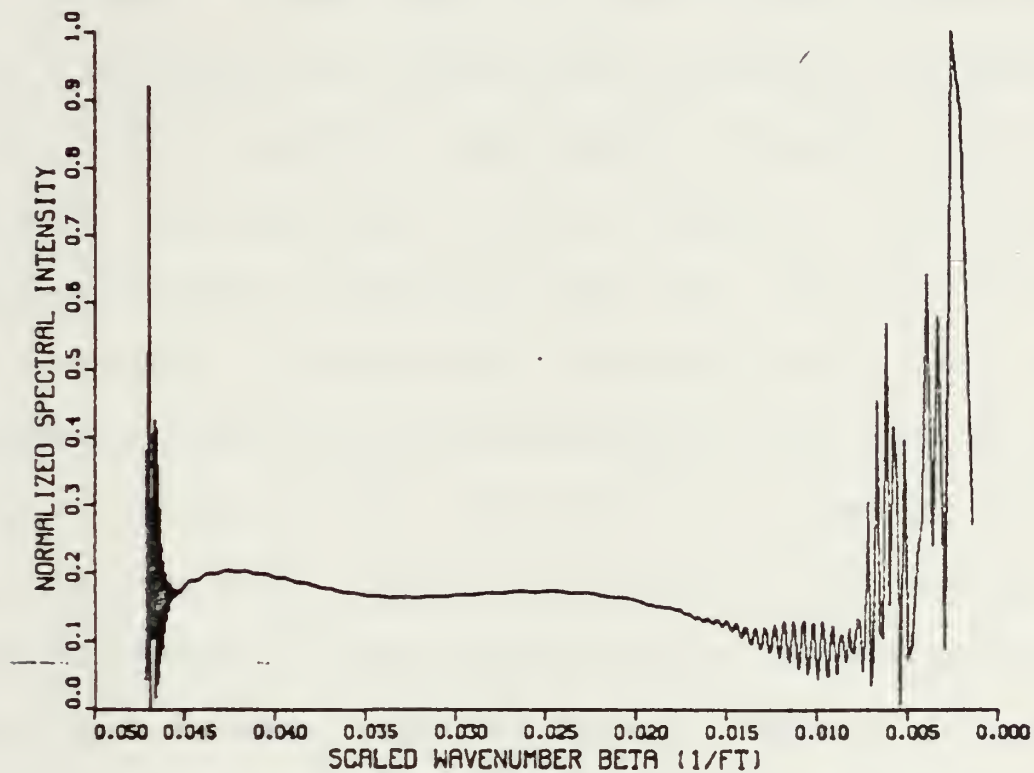SD:50FT RD:300FT F:100HZ Z:5000FT R:100NM

Figure 17.   Isospeed Profile Wavenumber Spectrum for SD of
50 ft.

cent intensity minima, such as shown in Figs. 5 through 16.
The nulls selected for measurement were those in the middle
of the spectrum, which led to a consistent technique for
comparison and avoided the rapidly decreasing null spacing
near the left intensity maxima. The distance was measured
to the nearest 1/64 of an inch and equated to the respective
null spacing. Thus, there is some inherent measurement
error. The exact null locations were difficult to determine
in the shallow isospeed cases because of gentle spectrum
curvature and uncertainty in null location. The actual
profiles were very complex and again the nulls were diffi-
cult to locate. One value for each spectrum plot was used
to generate a point on the determination curve, such as Fig.
18 for a series of runs. The variation of the data points
from the theoretical Lloyd's Mirror curve will be the normal
distance between the point and the curve. Measurement inac-
curacy will decrease as source depth increases. This will
be significant because at shallow depth there is some varia-
tion noted from sound speed differences. The nulls are
well-defined at great depths, but there is little variation
already, thus the measurement errors were not considered
significant. It is possible that a numerical algorithm which

could quantitatively identify the null locations could minimize this error.

This expectation is inferred from the wavenumber plots by Lauer (1979) and his examination of range determination. He found that range determination resolution increased as the distance between source and receiver decreased. It is possible that a similar relationship might exist for depth determination. Thus greater resolution may be realized at shallow source depth. Even at greater source depths the resolution may be acceptable for certain applications where an approximate depth is acceptable.

The prediction curves which result from the individual WT spectra will be discussed in following sections. Table III is a listing of the prediction curve comparisons which were conducted. In the figures only one symbol may appear at a source depth if both curves had the same null spacing value.
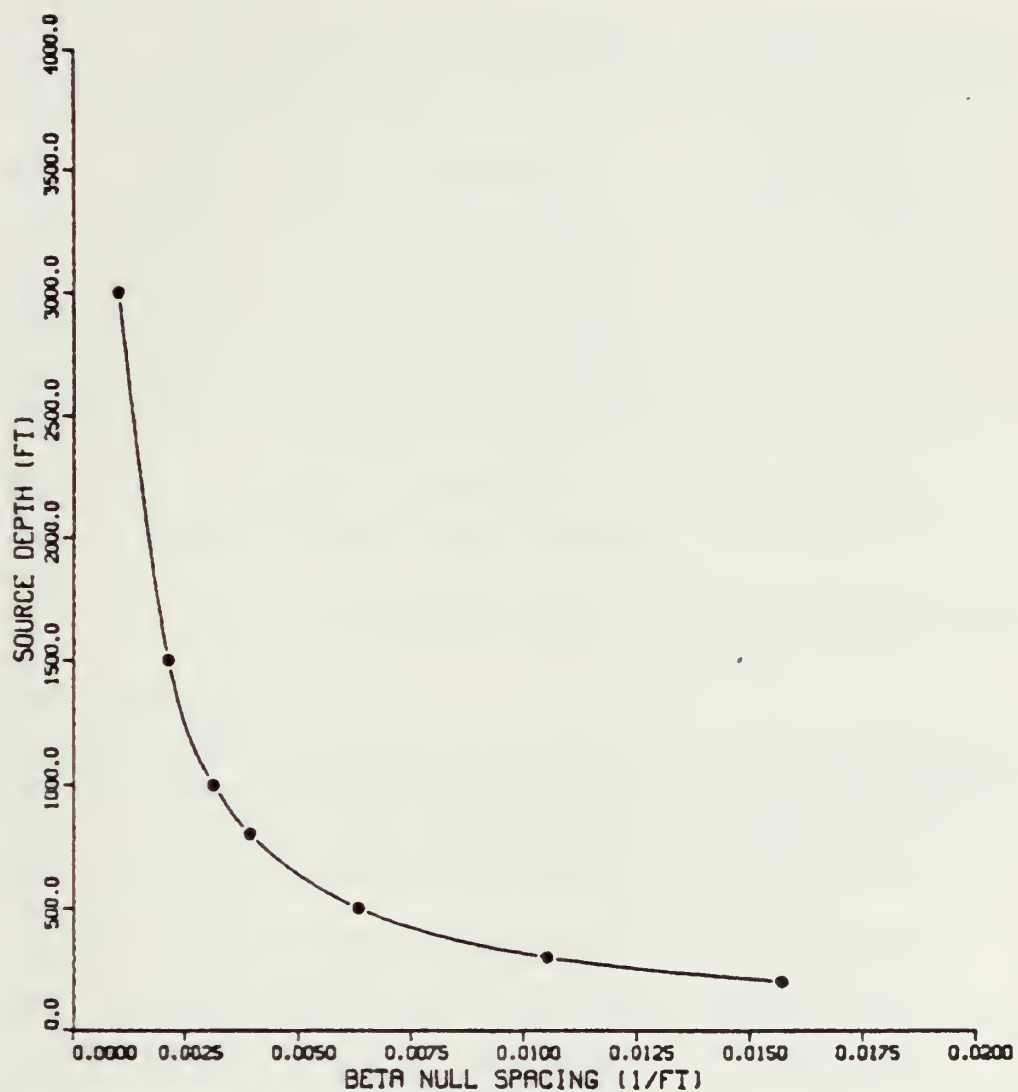
SOURCE DEPTH DETERMINATION CURVE

Figure 18.   Example of Source Depth Determination Curve.

TABLE I II
Comparison Specifications

ISOSPEED PROFILE

Figure	Run Sets	Constant Parameters	Varying Parameter
19	I1,I5	R:50,F:50,RD:300	Z:10000,5000 ft
20	I0,I3	R:50,F:100,RD:300	Z:10000,5000 ft
21	I2,I6	R:100,F:50,RD:300	Z:10000,5000 ft
22	I7,I4	R:100,F:100, RD:300	Z:10000,5000 ft
23	I5,I6	F:50,Z:5000,RD:300	R:50,100 nm
24	I1,I2	F:50,Z:10000,RD:300	R:50,100 nm
25	R1,R2,R3	F:100,Z:10000,RD:300	R:25,50,75 nm
26	I2,I7	R:100,Z:10000,RD:300	F:100,50 hz
27	I0,I1	R:50,Z:10000,RD:300	F:100,50 hz
28	I1,I8,I9	R:50,F:50,Z:10000	RD:300,800,10000 ft

REALISTIC PROFILE

Figure	Run Sets	Constant Parameters	Varying Parameter
29	A0,B0	R:100,F:100,RD:300	Space:200 nm
30	C0,D0	R:100,F:100,RD:300	Space:200 nm
31	A0,C0	R:100,F:100,RD:300	Time:20 days
32	B0,D0	R:100,F:100,RD:300	Time:20 days
33	A0,A3	F:100,16NOV,RD:300	R:100,50 nm
34	A0,A1,A2	F:100,16NOV, R:100	RD:300,1000,9000 ft

COMPOSITE

Figure	Run Sets	Constant Parameters	Varying Parameter
35	(All Isospeed and Actual Profile Run Sets)		

B. ISOSPEED CASES

1. Water Column Depth Variation

Fig. 19 is the comparison for a frequency of 50 Hz and a range of 50 nm at water column depths of 5000 and 10,000 feet. It was not expected that there would be any variation if the water column depth was modified, since all bottom interacting rays should be fully absorbed. The curves showed excellent agreement at source depths of 800 feet and greater, but there was some variation noted for 500 feet and shallower. Some variation may be related to measurement error, as noted above. Maximum variation from theory is observed for both depths in the middle depth range, approximately 500 feet, which is also the region of greatest curvature in the source depth determination curve.

Fig. 20 is the same except the frequency has been increased to 100 Hz. There is better agreement from 200 to 3000 feet; however, the significance of the frequency variation has not been evaluated. Fig. 21 is for a frequency of 50 Hz and a range of 100 nm, and Fig. 22 is for 100 Hz and 100 nm. Some variations are noted; however, they may not be significant, which would agree with the supposition that
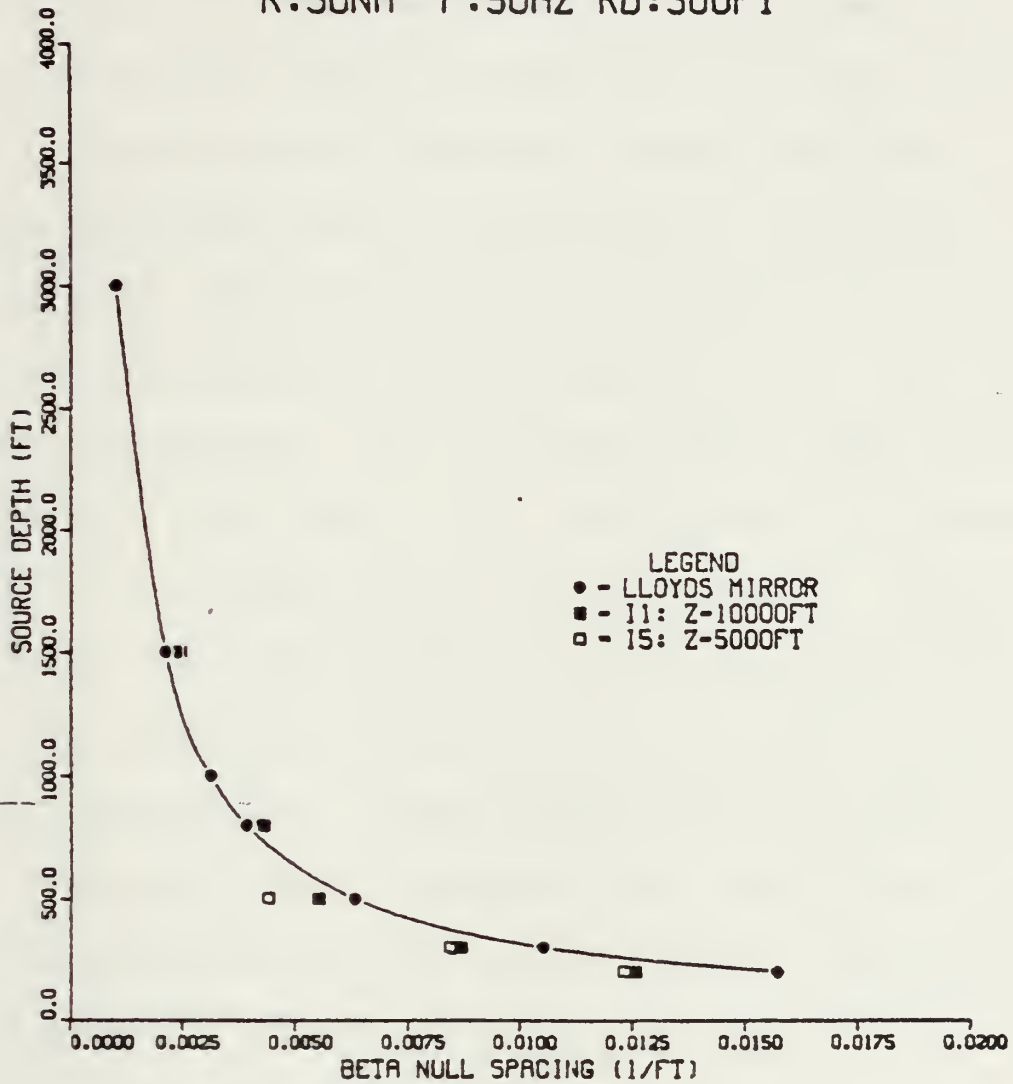
Figure 19. Isospeed Profile SD Determination Curve: Z Variation - 1.

water column depth differences will not be significant for an isospeed profile.

2. Range Variation

Fig. 23 is the comparison for a frequency of 50 Hz and a water column depth of 5000 feet for 50 and 100 nm. There is essentially no difference between the curves. The experimental curves agree well from 800 to 3000 feet, but once again the shallow variations may result from inaccuracies in evaluating beta from the spectrum plots. Fig. 24 is a similar comparison, but the water column depth has been increased to 10,000 feet. Fig. 25 increases the frequency to 100 Hz for ranges of 25, 50 and 75 miles. Again all curves show very good agreement with theory, which indicates that range variations within 100 nm of the source will probably be insignificant. Ranges beyond 100 nm were not tested since Fitzgerald (1975) suggested that the SSFFT was not a good approximation for 100 HZ beyond 111 km. This could be tested later.

3. Frequency Variation

Fig. 26 is the comparison for a range of 50 nm and a water column depth of 5000 feet for 50 and 100 Hz. Both curves agree well with theory below 800 feet, but at 500

SOURCE DEPTH DETERMINATION CURVE
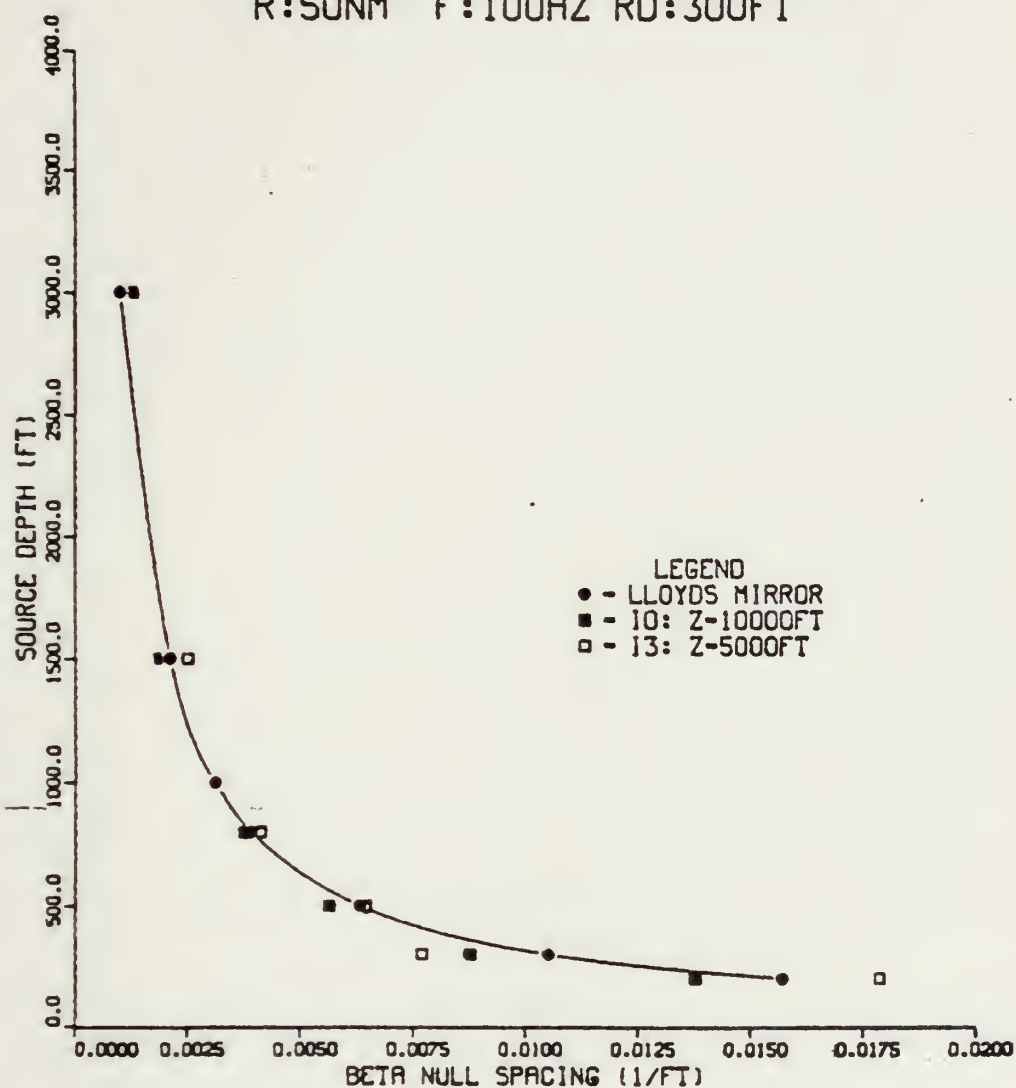ISOSPEED WATER DEPTH VARIATION
R:50NM   F:100HZ RD:300FT

LEGEND
● - LLOYDS MIRROR
■ - IO: Z-10000FT
□ - I3: Z-5000FT

Figure 20.   Isospeed Profile SD Determination Curve: Z
              Variation - 2.

90

SOURCE DEPTH DETERMINATION CURVE
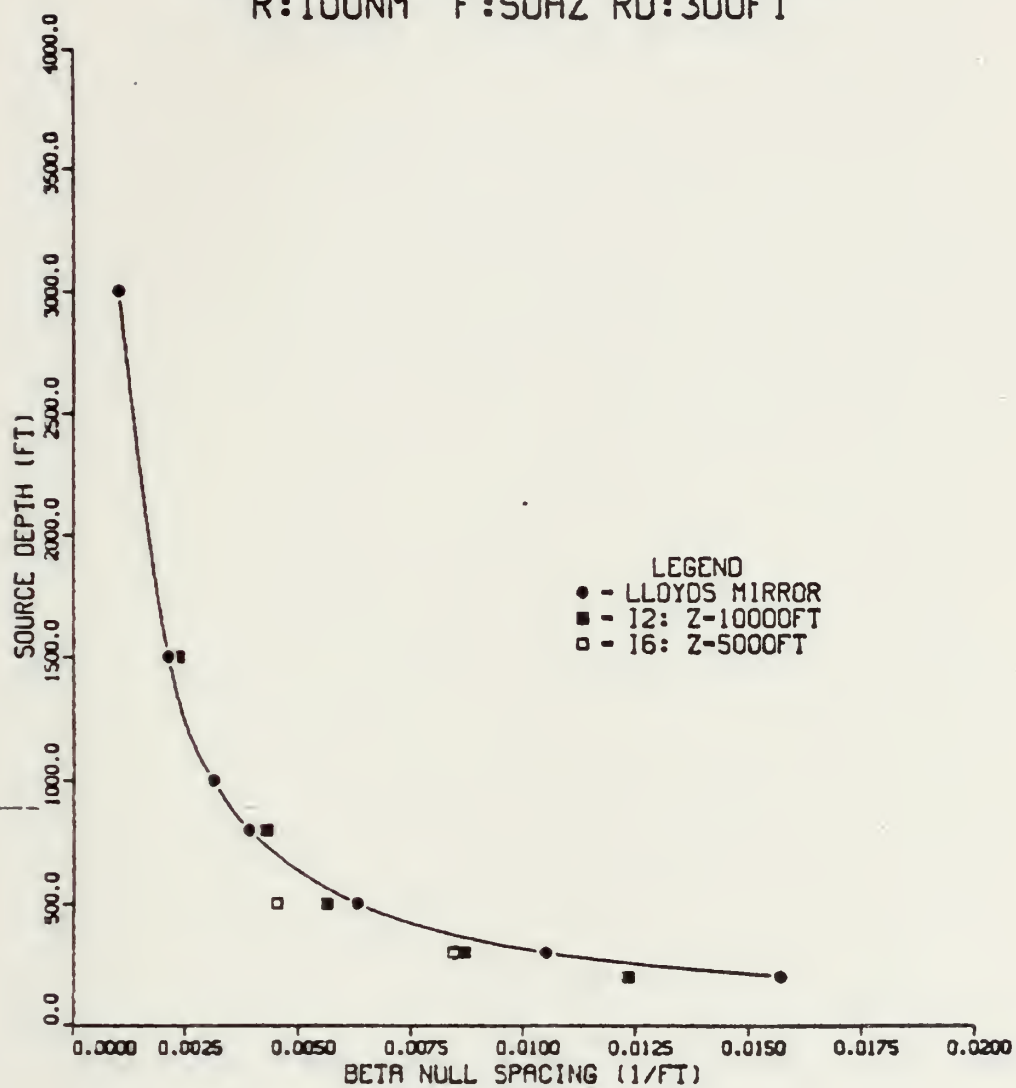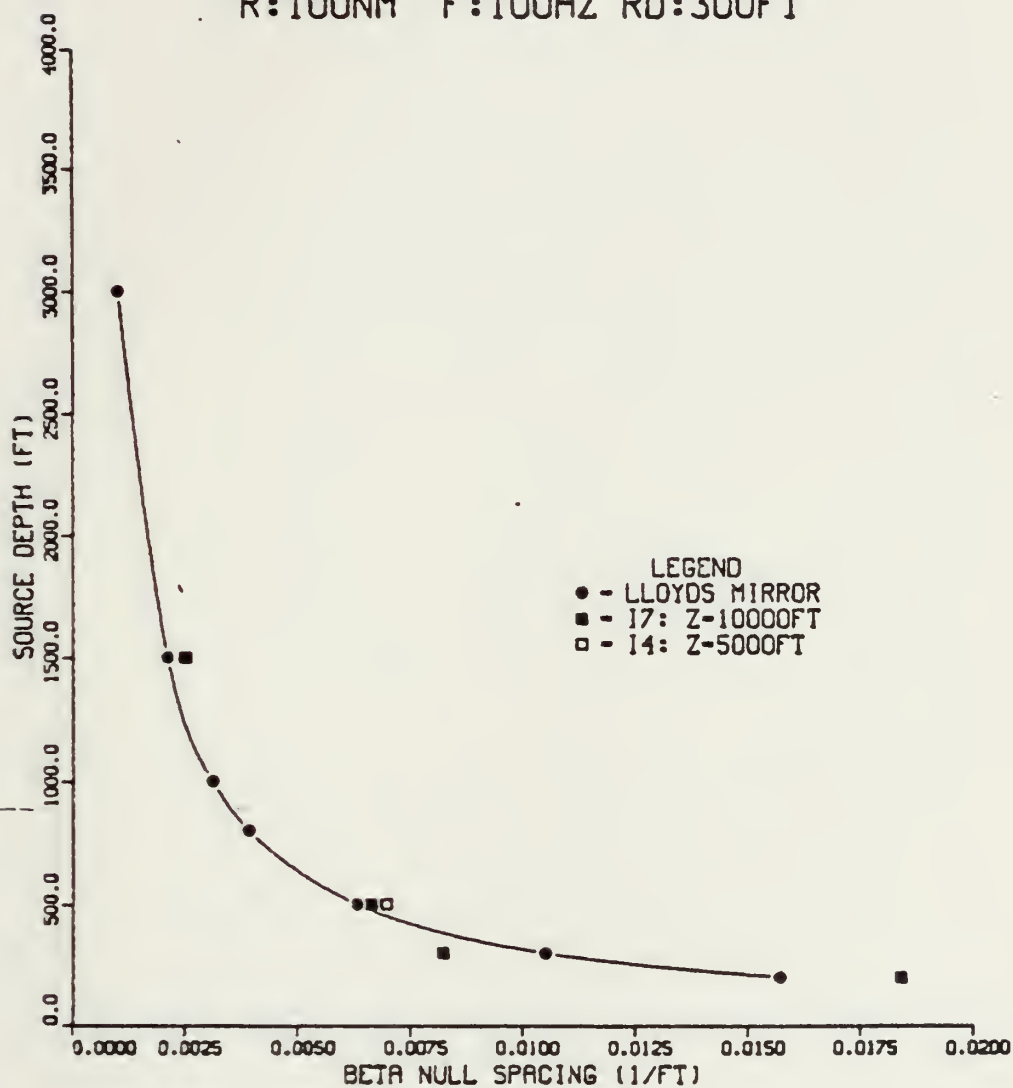ISOSPEED WATER DEPTH VARIATION
R:100NM F:50HZ RD:300FT

LEGEND
● - LLOYDS MIRROR
■ - I2: Z-10000FT
□ - I6: Z-5000FT

Figure 21.   Isospeed Profile SD Determination Curve: Z
             Variation - 3.

SOURCE DEPTH DETERMINATION CURVE
ISOSPEED WATER DEPTH VARIATION
R:100NM F:100HZ RD:300FT

LEGEND
● - LLOYDS MIRROR
■ - 17: Z-10000FT
□ - 14: Z-5000FT

Figure 22.   Isospeed Profile SD Determination Curve: Z
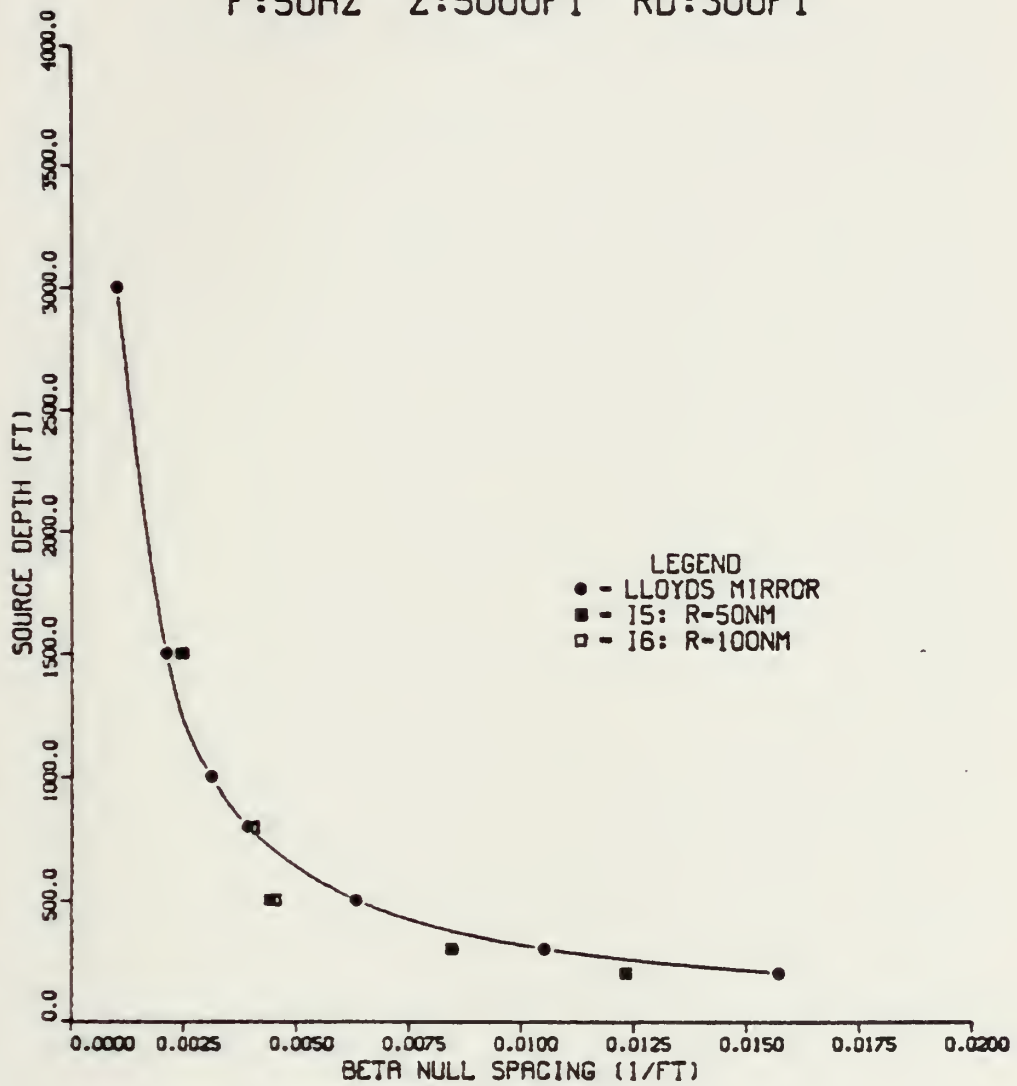   Variation - 4.

92

Figure 23.   Isospeed Profile SD Determination Curve: R
             Variation - 1.

93

SOURCE DEPTH DETERMINATION CURVE
ISOSPEED RANGE VARIATION
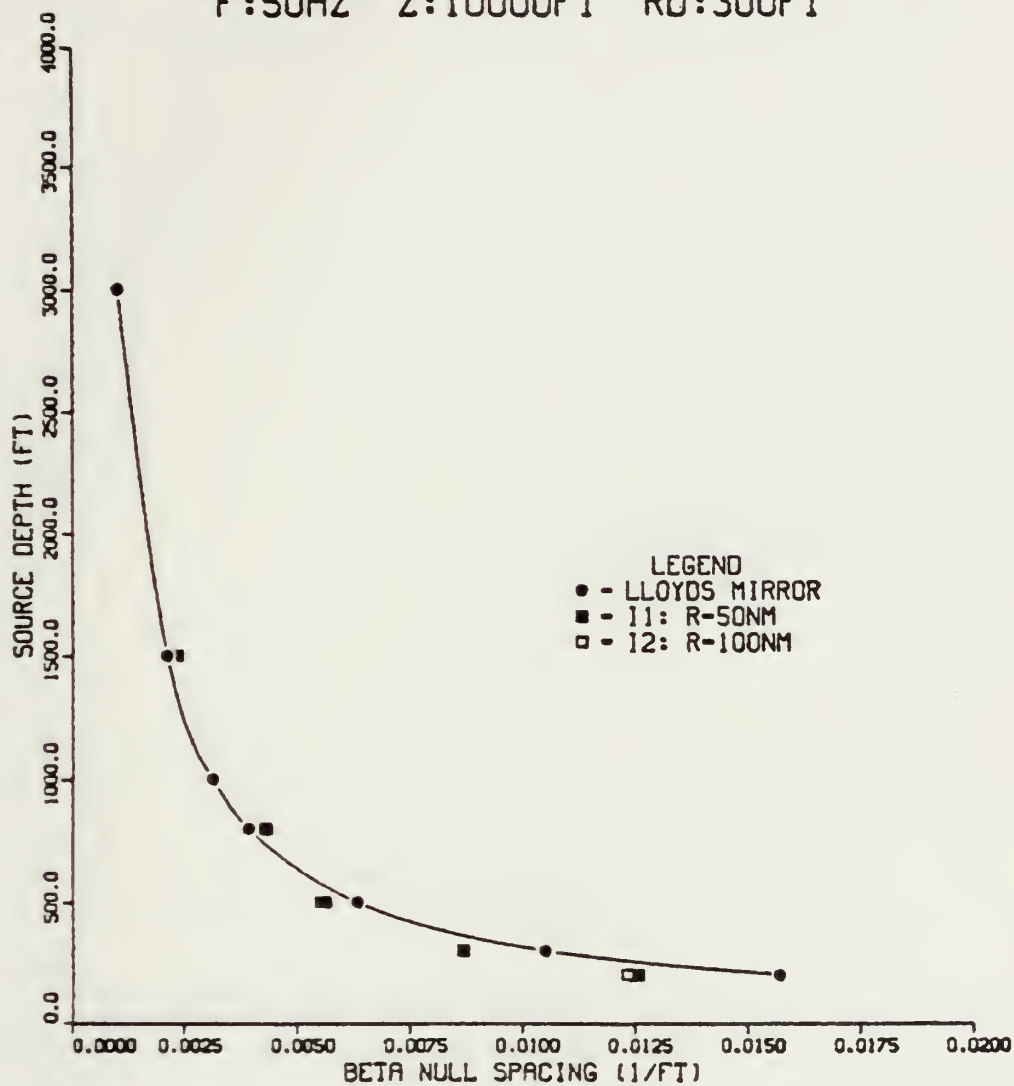F:50HZ Z:10000FT RD:300FT

Figure 24. Isospeed Profile SD Determination Curve: R
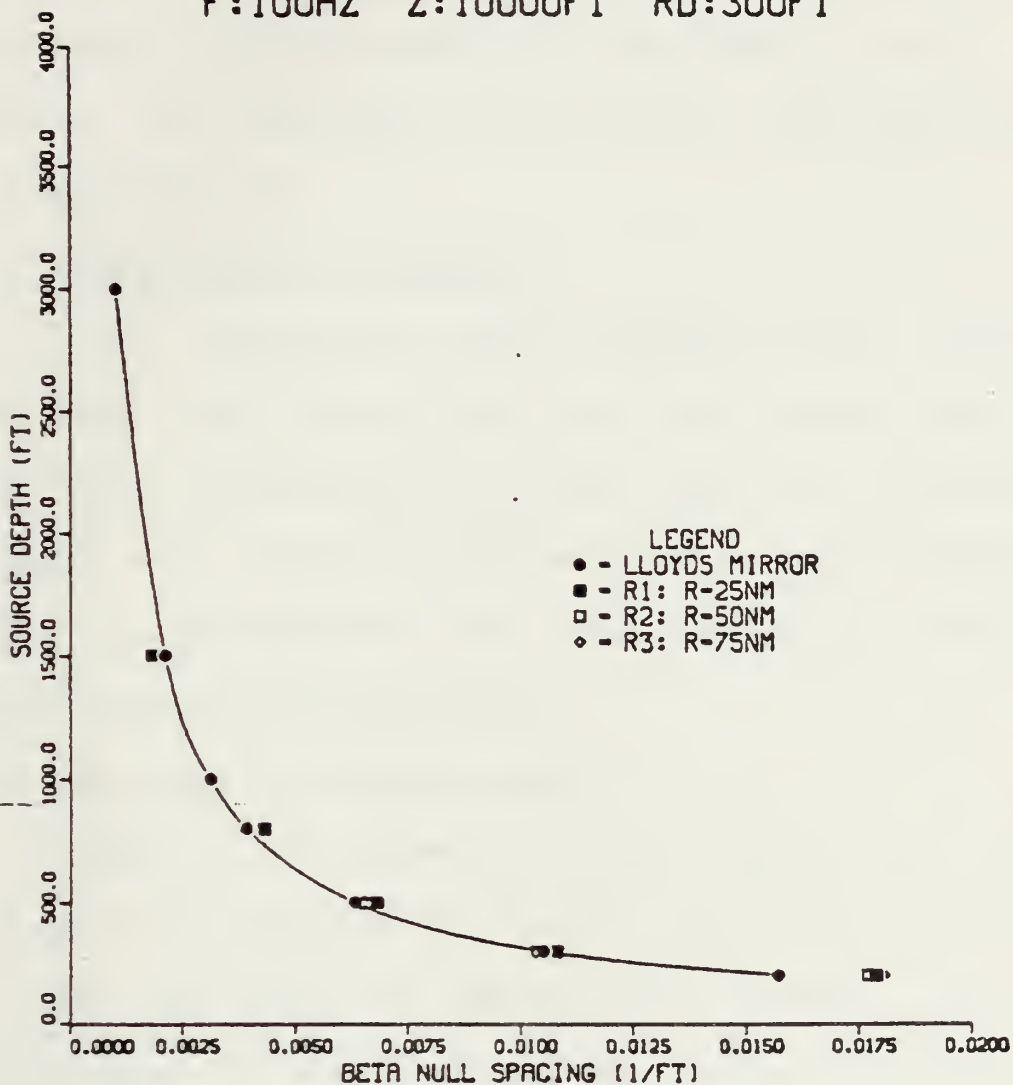   Variation - 2.

Figure 25.   Isospeed Profile SD Determination Curve: R
Variation - 3.

feet the higher frequency appears to agree better. Fig. 27
extends the water column depth to 10,000 feet and there is
apparently better agreement with the theoretical curve.
Overall there appears to be better agreement at 100 Hz than
at 50 Hz, but this result is not certain with the limited
number of cases run.

4. Receiver Depth Variation

Fig. 28 compares receiver depths of 300, 800 and
10,000 feet for a range of 50 nm, water column depth of
10,000 feet, and frequency of 50 Hz. Again all curves agree
reasonably well. There is perhaps slightly better agreement
for the shallow receiver, but this supposition cannot be
verified from these limited data.

5. Analysis of Isospeed Cases

There do not appear to be any significant differ-
ences for water column depth, range, frequency or receiver
depth over the limits of variations considered. This was
expected since the theory is supposed to be only a function
of source depth for an isospeed profile. Thus the WT would
be expected to be equally effective for various transmis-
sion geometry patterns and frequencies, if the sound speed
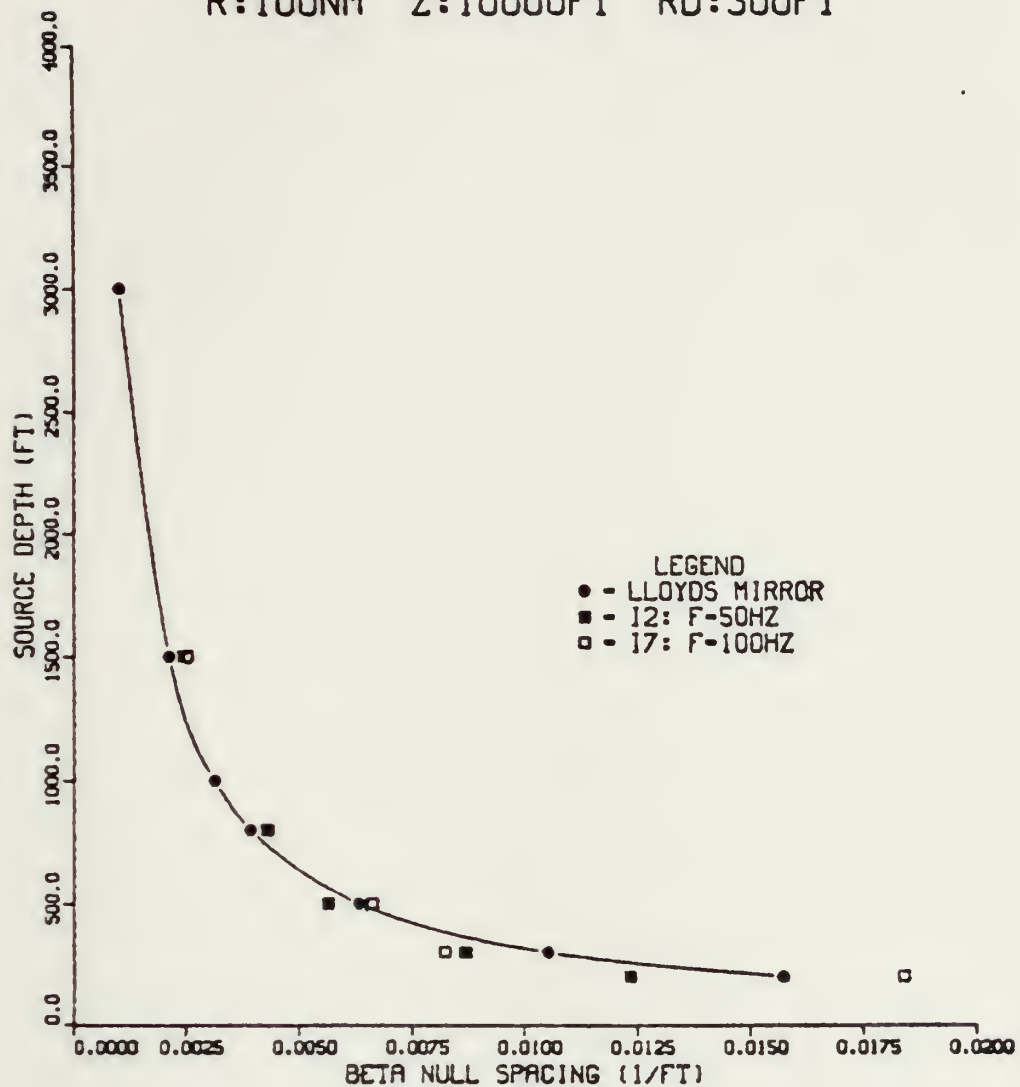profile is constant and the bottom fully absorptive. There

Figure 26. Isospeed Profile SD Determination Curve: F
            Variation -1.

SOURCE DEPTH DETERMINATION CURVE
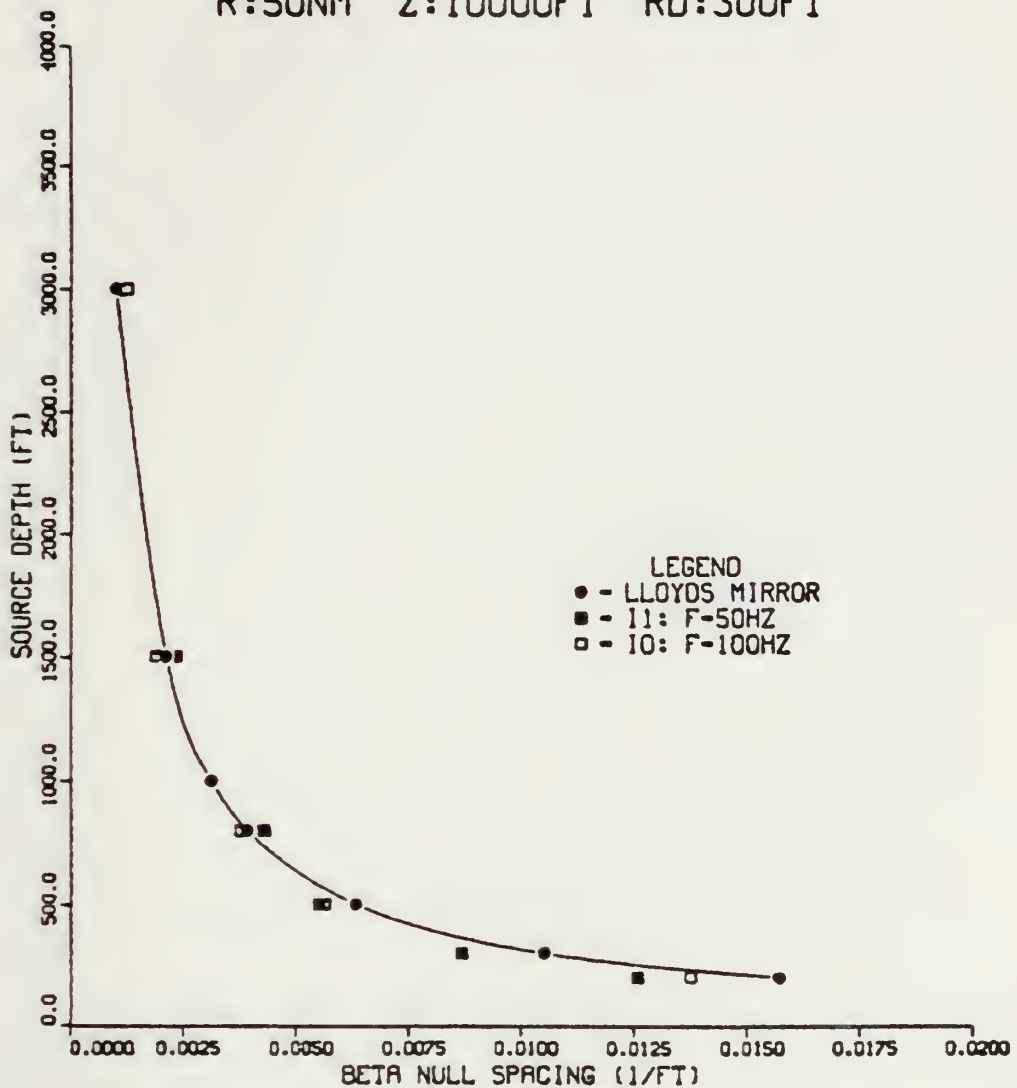ISOSPEED FREQUENCY VARIATION
R:50NM Z:10000FT RD:300FT

Figure 27.   Isospeed Profile SD Determination Curve: F
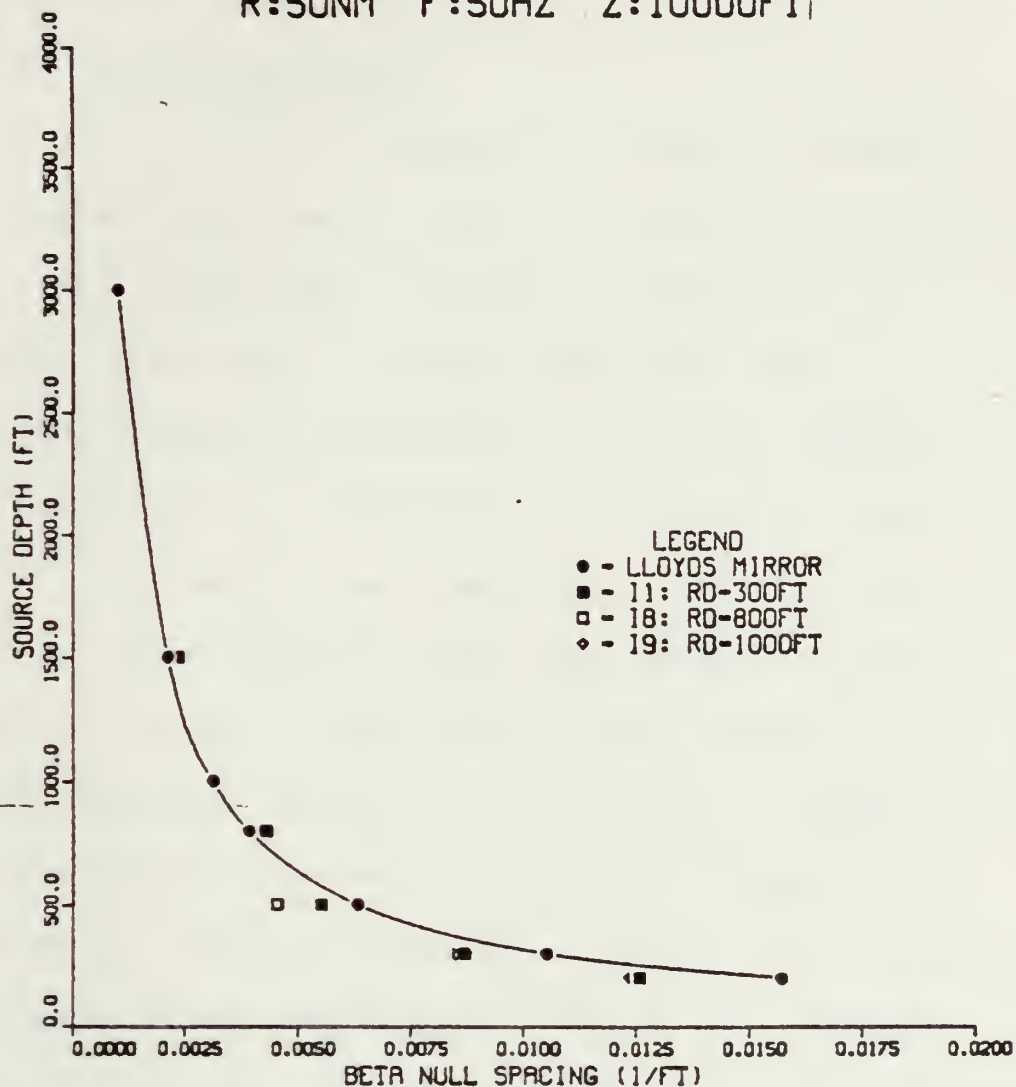   Variation -2.

Figure 28. Isospeed Profile SD Determination Curve: RD Variation.

99

may be slight effects for receiver depth and frequency, but these have not been substantiated.

C. REALISTIC PROFILE CASES

1. Spatial Variation

Fig. 29 is the comparison of spatial variability for the curves which resulted from the spectra of profiles A and B. (The sound speed profiles corresponding to the prediction curves will be included for each comparison.) These were both sampled on November 16, 1980, and represent a spatial separation of about 200 nm. Both profiles result in a slight bias below the theoretical Lloyd's Mirror curve. There is more variation along each curve, which is to be expected because the profiles are not isospeed. Also, partially absorbing bottoms are now used as compared to the fully absorbing bottoms used with the isospeed cases. The profile and bottom effects have not yet been separated to determine which contributes more to the departure from theory. This would require an extensive set of intercomparisons between these two parameters. (The present intent is to show that ocean variability is important.) It is difficult to differentiate between the two curves, but it appears that there is a slight trend in B toward smaller null

spacings. Sound speed profile B is slower than A over the entire depth. A slower sound speed would appear to indicate that a ray of lesser angle would be required to provide the second arrival for the interference pattern. That would correspond to a greater vertical wavenumber and decreased beta null spacing.

Fig. 30 compares profiles C and D, which were sampled at the same locations as profiles A and B, respectively, but on December 6, 1980. A similar pattern is noted with D spacing less than C, which may again correspond to slower sound speeds for profile D.

2. Temporal Variation

Fig. 31 compares profiles A and C which represent the same location, but a separation of 20 days. There appears to be a curve crossing at about 800 feet, such that spacing is less at A for shallow depths and greater for A below 800 feet. The A sound spped profile is slower than the C profile down to 800 feet and the pattern is reversed from 800 to 2000 feet. Slower speeds appear to be related to shorter null spacings, which appears consistent with this example. The variations between the curves, however, are quite small.

SOURCE DEPTH DETERMINATION CURVE
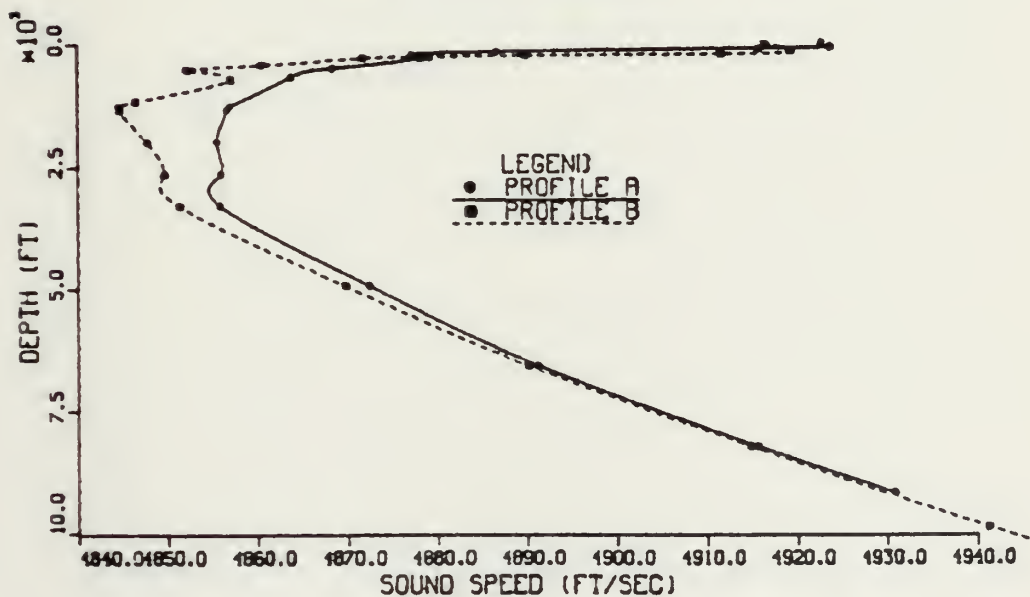## REALISTIC SPATIAL VARIATION
F:100HZ   R:100NM   RD:300FT
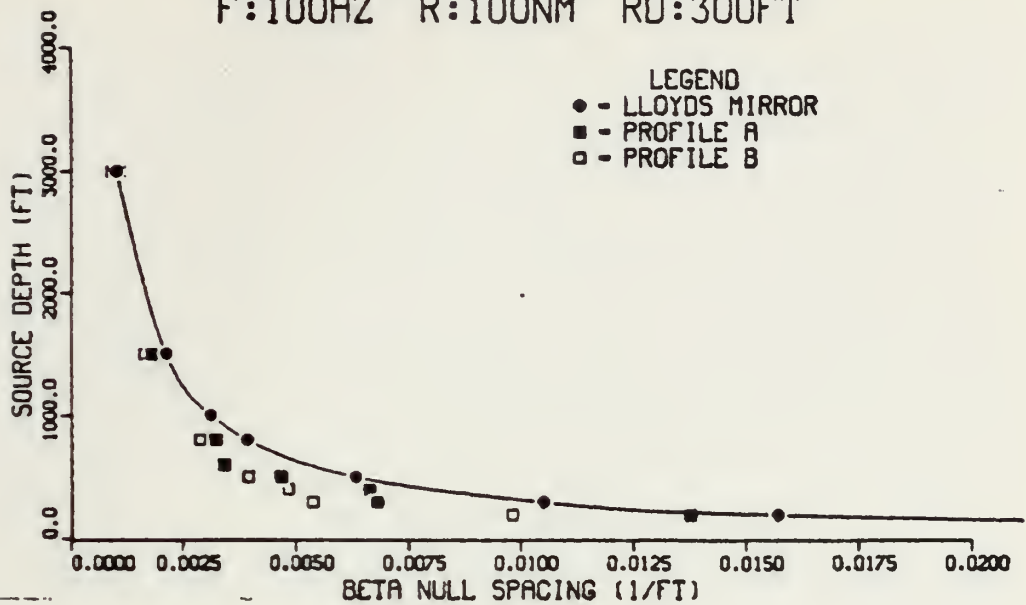
AXBT CURVES

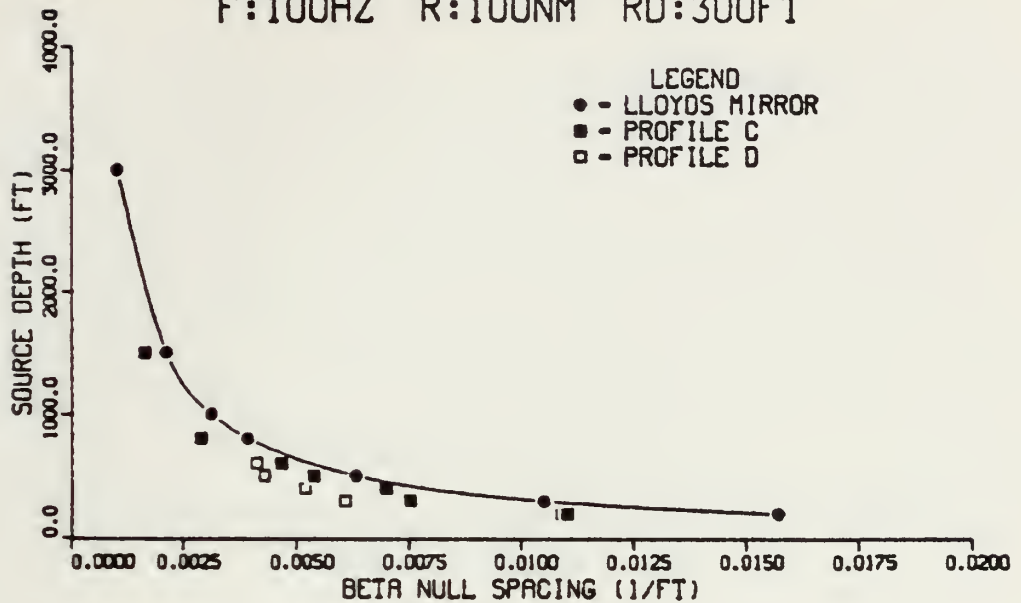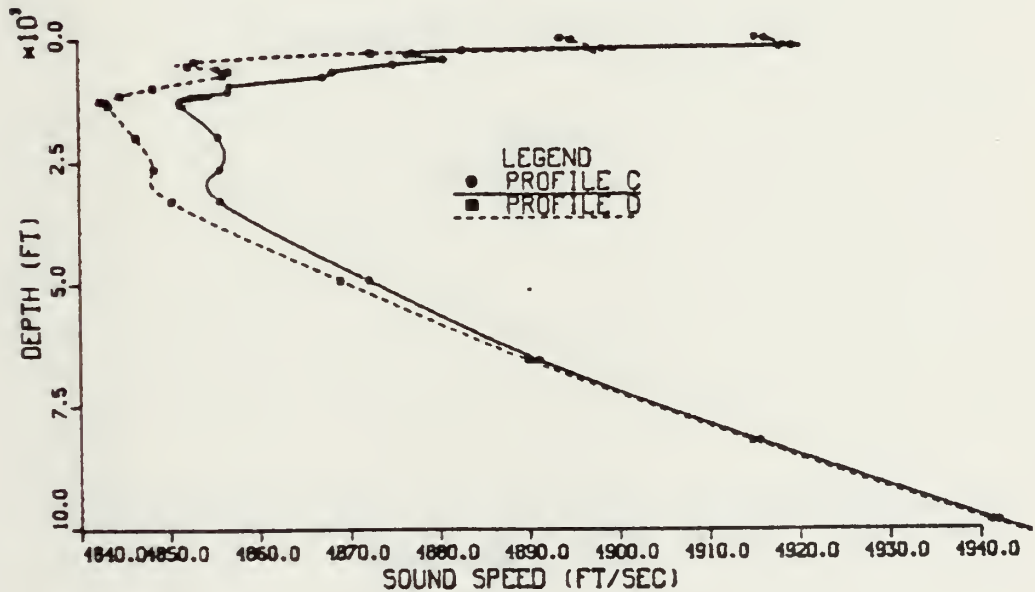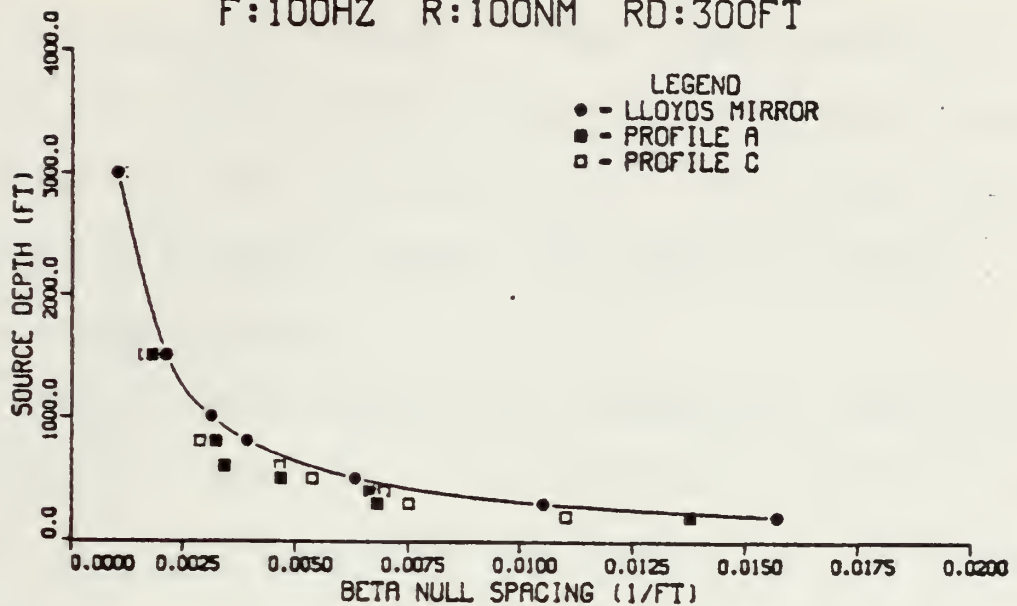Figure 29.   Spatial Variation (A,B): SD Determination and AXBT Curves.

102

Figure 30. Spatial Variation (C,D): SD Determination and AXBT Curves.

SOURCE DEPTH DETERMINATION CURVE
REALISTIC TEMPORAL VARIATION
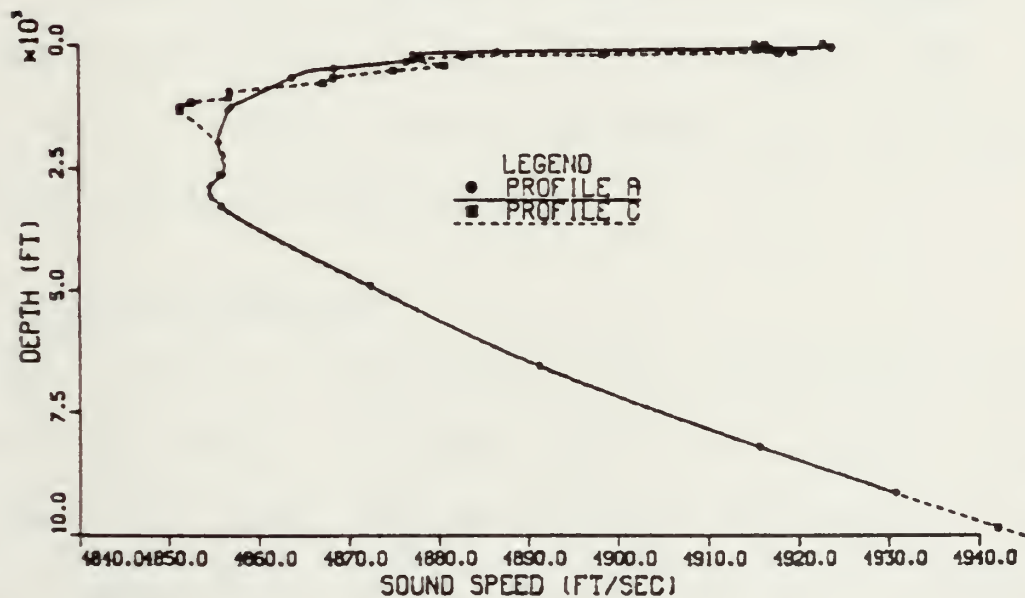### F:100HZ R:100NM RD:300FT

AXBT CURVES

Figure 31. Temporal Variation (A,C): SD Determination and
AXBT Curves.

Fig. 32 presents a similar comparison for profiles B and D. The speed profiles show almost no differences, except that D is slightly slower. This result appears as a slightly sharper deep sound channel which will mean slightly slower velocity for the direct path. That effect may be reflected as a slightly greater null spacing as shown.

3. Range Variation

Results for profile A were compared for ranges of 50 and 100 nm in Fig. 33. No significant variations were noted, which is similar to the results for the isospeed cases.

4. Receiver Depth Variation

Results for profile A were also compared for receiver depths of 300, 1000 and 9000 feet in Fig. 34. There may be slightly better agreement for the shallow receiver, but this is not certain.

D. COMPOSITE COMPARISON

Fig. 35 is a composite of all isospeed and actual profile data sets. Isospeed data show slightly better agreement with theory; however realistic profiles are a reasonable approximation to the theoretical curve. Realistic profile variations from the isospeed curve appear to be

related to the sound speed profile and different bottom boundary conditions. The general relationships of the data indicate that below about 800 feet no significant variations are noted. Specific curves will apparently provide better predictions at shallower depths. It may be sufficient for certain applications to provide climatological or theoretical prediction curves. These curves could be enhanced or modified by updated curves that would reflect the current sound speed profile.

SOURCE DEPTH DETERMINATION CURVE
REALISTIC TEMPORAL VARIATION
F:100HZ R:100NM RD:300FT
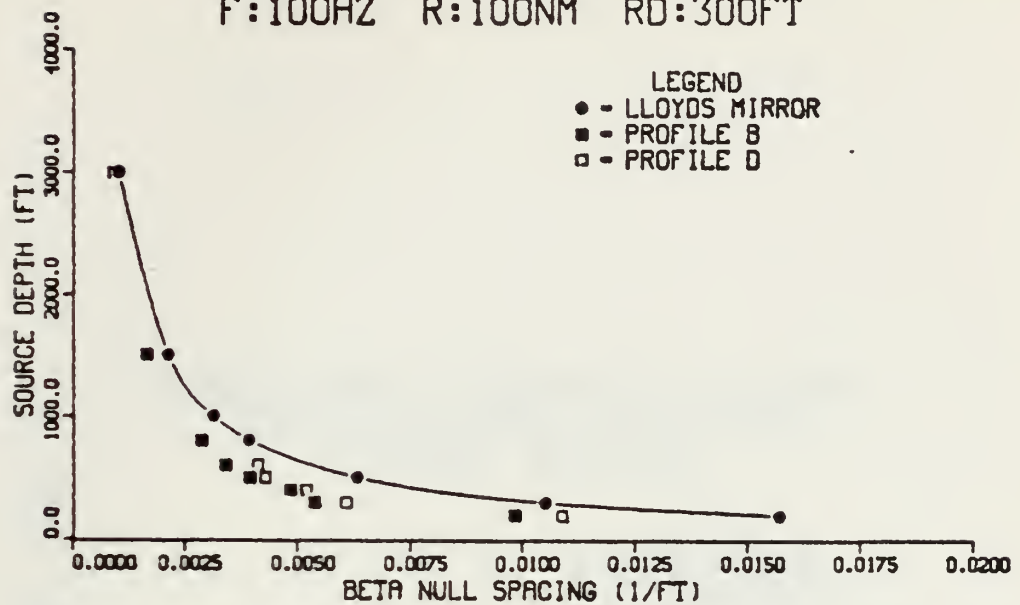
AXBT CURVES

Figure 32.   Temporal Variation (B,D): SD Determination and AXBT Curves.
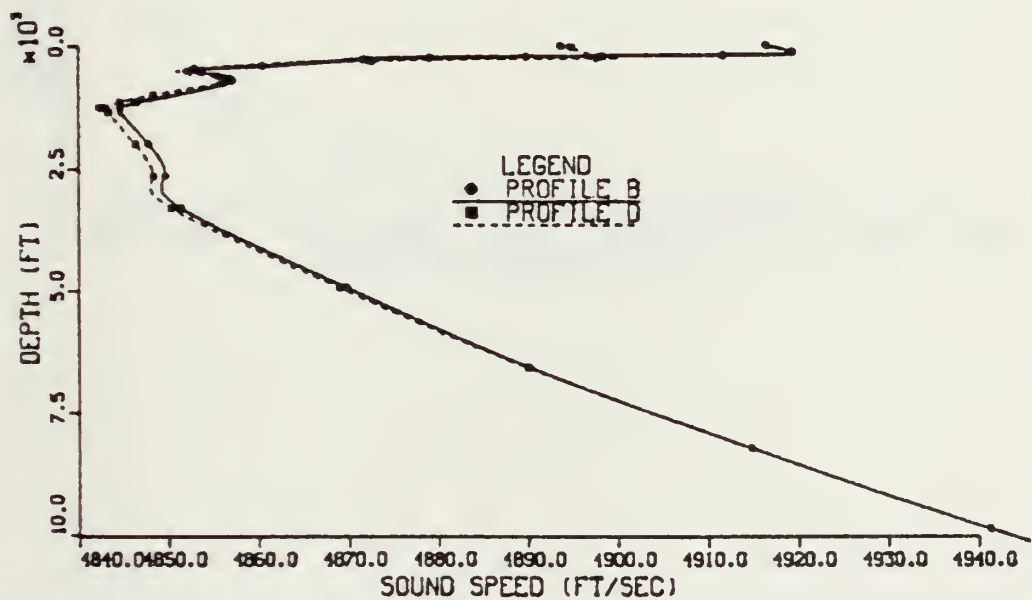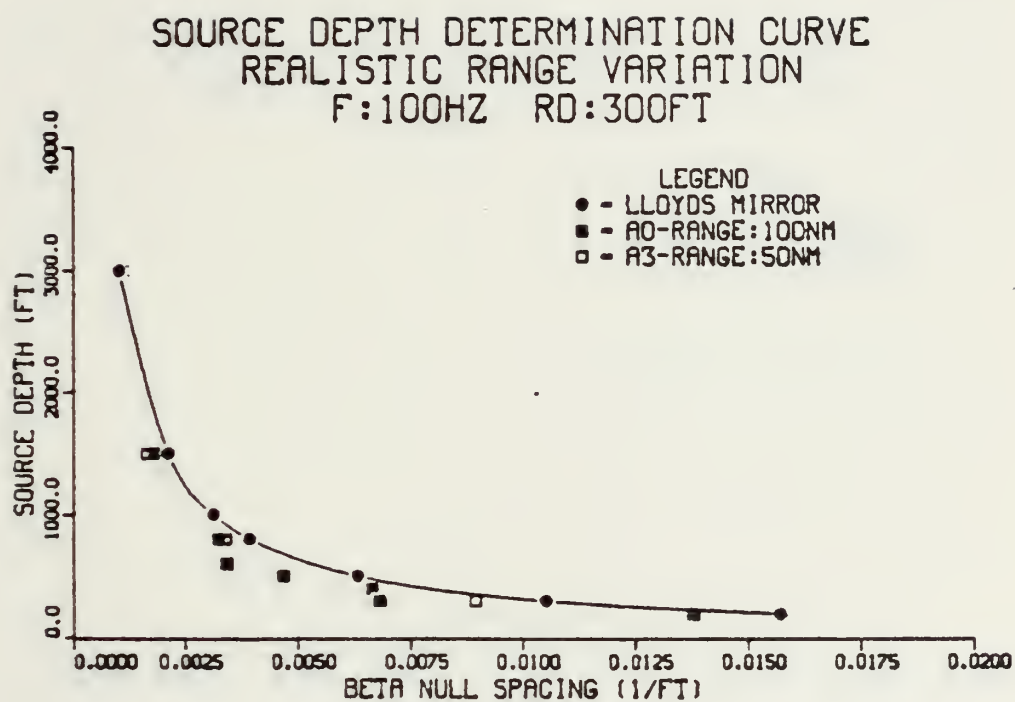
107

Figure 33.   Range (R) Variation for Profile A.
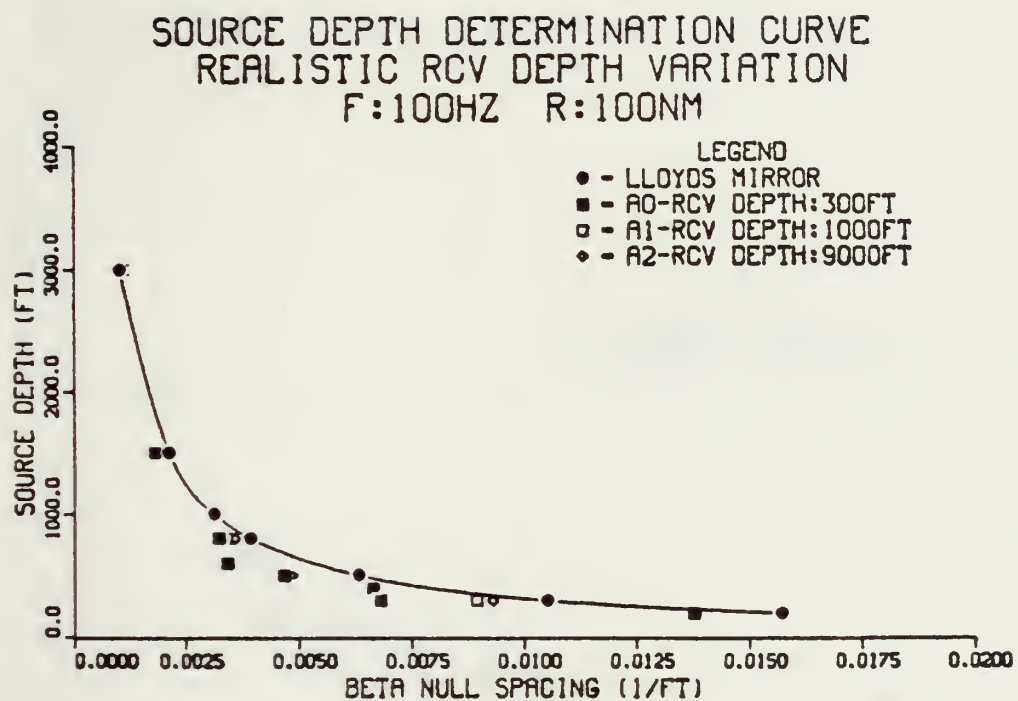
Figure 34. Receiver Depth (RD) Variation for Profile A.

Figure 35. Composite Comparison for Isospeed and Realistic Cases.

V. CONCLUSIONS

The Wavenumber Technique (WT), as proposed by Lauer (1979) has been investigated for source depth determination. Several idealized and actual scenarios of oceanic and acoustic parametric variations were tested. There is excellent agreement between the ideal test cases and the theoretical Lloyd's Mirror effect. The realistic cases showed significant similarity as well, but with some bias toward smaller wavenumber spacing. This is qualitatively attributed to sound speed profile variations in the water and sediment.

There appears to be a response of the WT to variations in input, which is beneficial in allowing evaluation of the relative importance of individual parameters. Changes in range and water column depth do not indicate any significant variation. Some differences are possibly suggested for receiver depth and frequency, but the results have not been fully analyzed. The WT appears to respond well to changes in the environmental parameters, such as sound speed profile. This is seen from the average bias of the actual cases from the isospeed cases. The bias does appear to be

111

relatively consistent and shows the importance of oceanic variations in both space and in time. Thus, it appears that, if information is available for the bottom structure, and if a realistic sound speed profile can be generated, then a very specific family of curves could be generated for various frequency and receiver depth combinations. This simplicity indicates possible operational applicability and flexibility.

These are the first known source depth determination curves for the WT and thus there is no comparison available. It may be that there are some biases in these curves which would be discovered when comparative runs are made using other inputs or propagation models. Comparison with observed signals might also reveal biases that are related to the WT or to the propagation model. An explanation has not been determined for the U-shape nature of the wavenumber spectrum plots and thus slightly different curves might result if this is found to bias the null spacing. Also there is a bias associated with the method of manually estimating the null spacing. This might be resolved with a computer procedure to locate the nulls. The experimental curves actually agree well with theory under the assumption of a flat,

totally-reflecting surface and a fully-absorbing bottom. The premise that the theory might be approximately accurate in realistic cases appears valid. This overall generally smooth fit supports the validity of the WT.

This has been an initial investigation of the WT, and thus only a broadbrush study was possible. These preliminary results indicate that additional analysis might be beneficial. The response of the WT to input from different propagation models would determine if results from different models could be compared. Detailed investigation of the specific effects of various parameters would lead to a quantitative analysis of the sensitivity of the WT. An explanation for the anomalous U-shaped spectrum and the development of an algorithm which can accurately determine null locations would be necessary before the WT could be used practically. An extremely important investigation would be the comparison of analyzed actual signals to predictions from the WT to determine applicability, accuracy, consistency and any appropriate biases.

The intent of this research was to determine the validity of the WT by development of source depth determination curves and to evaluate the oceanic and acoustic

sensitivities of these curves. The results obtained indicate that in general the WT appears to be valid with respect to the Lloyd's Mirror effect. The parametric variations which were investigated show that oceanic variability is extremely important, but that the WT is flexible for other parameters, such as transmission geometry. The WT appears to be viable for operational applications. The additional investigations suggested above would determine the validity of this supposition. It is conceivable that the WT could be developed into an operational prediction product.

LIST OF REFERENCES

Brock, H.K., Buchal, R.N., and Spofford, C.W.,"Modifying the Sound Speed Profile to Improve the Accuracy of the Parabolic-Equation Technique," J. Acoust. Soc. Am.,v. 62, p.543-552, September 1977.

DeSanto, J.A., "Relation between the Solutions of the Helmholtz and Parabolic Equations for Sound Propagation," J. Acoust. Soc. Am., v. 62. p. 295-297, August 1977.

DeSanto, J.A., Perkins, J.S., and Baer, R.N., "A Correction to the Parabolic Approximation," J. Acoust. Soc. Am., v. 64, p. 1664-1666, December 1978.

DiNapoli, F.R. and Deavenport, R.L., "Numerical Models of Underwater Acoustic Propagation," in Ocean Acoustics, ed. by J.A. DeSanto, Springer-Verlag, 1979, p. 79-158.

Dunlap, C.R., "Naval Postgraduate School ASTREX Measurements," (Unpublished), 1982.

Fitzgerald, R.M., "Helmholtz Equation as an Initial Value Problem with Application to Acoustic Propagation," J. Acoust. Soc. Am., v. 57, p. 839-842, April 1975.

Hardin, R.H. and Tappert, F.D., "Applications of the Split-Step Fourier Method to the Numerical Solution of Nonlinear and Variable Coefficient Wave Equation," SIAM Review, v. 15, p. 423, 1973.

Kinsler, L.E., Frey, A.R., Coppens, A.B. and Sanders, J.V., Fundamentals of Acoustics, Third Edition, John Wiley and Sons, 1982.

Lauer, R.B. (1), Personal communication to B.B. Stamey on October 22, 1982.

Lauer, R.B. (2), Personal communication to B.B. Stamey on December 16, 1982.

Lee, D., Botseas, G., and Papadakis, J.S., "Finite-Difference Solution to the Parabolice Wave Equation," J. Acoust. Soc. Am., v. 70, p. 795-800, September 1981.

Leontovich, M.A. and Fock, V.A., "Solution of the Problem of Propagation of Electromagnetic Waves along the Earth's Surface by the Method of Parabolic Equation," J. Phys. of USSR, v. 10, p. 13, 1946.

McDaniel, S.T. (1), "Propagation of Normal Mode in the Parabolic Approximation," J. Acoust. Soc. Am., v. 57, p. 307-311, February 1975.

McDaniel, S.T. (2), "Parabolic Approximations for Underwater Sound Propagation," J. Acoust. Soc. Am., v. 58, p. 1179-1185, December 1975.

McDaniel, S.T. and Lee, D., "A Finite-Difference Treatment of Interface Conditions for the Parabolic Wave Equation: The Horizontal Interface," J. Acoust. Soc. Am., v. 71, p. 855-858, April 1982.

Naval Air Development Center Report NADC-72001-AE, Normal Mode Solutions and Computer Programs for Underwater Sound Propagation, by C. Bartberger and L. Ackler, 4 April 1973.

Naval Oceanographic Office Reference Publication 16, Regional Geologic Maps of the Northeast Pacific by W.T. Mortch and A. Lourie, 1978.

Naval Ocean Research and Development Activity Technical Note 12, The AESD Parabolic Equation Model, by H.K. Brock, January, 1978.

Naval Underwater Systems Center Technical Report 4103, Fast Field Program for Multilayered Media, by F.R. DiNapoli, 26 August 1971.

Naval Underwater Systems Center Technical Memorandum 771160, The Inverse Fast Field Program (IFFP): An Application to the Determination of the Acoustic Parameters of the Ocean Bottom, by F.R. DiNapoli, 5 August 1977.

Naval Underwater Systems Center Technical Report 4887-1, A Shallow Water Acoustic Model for an Ocean Stratified in Range and Depth, by W.G. Kanabis, 1975.

Naval Underwater Systems Center Technical Memorandum 791105, Signal Transmission in the Wavenumber Domain, by R.B. Lauer, 5 June 1979.

Naval Underwater Systems Center Technical Report 5929, Numerical Solutions of Underwater Acoustic Wave Propagation Problems, by D. Lee and J.S. Papadakis, February 1979.

Naval Underwater Systems Center Technical Report 6659, IFD: An Implicit Finite-Difference Computer Model for Solving the Parabolic Equation, by D. Lee and G. Botseas, 27 May 1982.

Officer, C.B., Introduction to the Theory of Sound Transmission with Application to the Ocean, McGraw-Hill, 1958.

Palmer, D.R., "Eikonal Approximation and the Parabolic Equation," J. Acoust. Soc. Am., v. 60, p. 343-354, August 1976.

Stieglitz, R., Dozier, L., Garon, H.M., and Spofford, C.W., Incorporation of an Ocean Bottom into the Parabolic Equation (PE) Algorithm, SAI-79-878-WA, Science Applications, Inc., McClean, Virginia, January 1979.

Tappert, F.D., "The Parabolic Approximation Method," in Wave Propagation and Underwater Acoustics, ed. by J.B. Keller and J.S. Papadakis, Springer-Verlag, 1977.

Tatro, P.R., Communication to Rowland M. Stevens, The Johns Hopkins University, on April 20, 1977.

Thorp, W.H., "Analytic Description of the Low Frequency Attenuation Coefficient," J. Acoust. Soc. Am., v. 42, p.270, July 1967.

Urick, R.J., Principles of Underwater Sound, Second Edition, McGraw-Hill, 1975.

Urick, R.J., Sound Propagation in the Sea, Defense Advanced Research Projects Agency, 1979.

INITIAL DISTRIBUTION LIST

No. Copies

1. Defense Technical Information Center   2
    Cameron Station
    Alexandria, VA 22314

2. Superintendent   2
    Attn: Library, Code 0142
    Naval Postgraduate School
    Monterey, CA 93940

3. Superintendent   1
    Attn: Professor C.N.K. Mooers, Code 68
    Naval Postgraduate School
    Monterey, CA 93940

4. Superintendent   1
    Attn: Professor R.J. Renard, Code 63
    Naval Postgraduate School
    Monterey, CA 93940

5. Superintendent   3
    Attn: Associate Professor A.B. Coppens, Code 61
    Naval Postgraduate School
    Monterey, CA 93940

6. Superintendent   3
    Attn: LCDR C.R. Dunlap, USN (Ret), Code 68
    Naval Postgraduate School
    Monterey, CA 93940

7. Commanding Officer   1
    Naval Ocean Research and Development Activity
    NSTL Station
    Bay St. Louis, MS 39522

8. Commanding Officer   2
    Attn: Mr. R.B. Lauer, Code 323
    Naval Ocean Research and Development Activity
    NSTL Station
    Bay St. Louis, MS 39522

9. Commanding Officer   2
    Attn: Mr. T.N. Lawrence, Code 323
    Naval Ocean Research and Development Activity
    NSTL Station
    Bay St. Louis, MS 39522

10. Commanding Officer   1
    Attn: Code 520
    Naval Ocean Research and Development Activity
    NSTL Station
    Bay St. Louis, MS 39522

11.   Commanding Officer   1
      Attn: CDR M. McCallister, USN, Code 522
      Naval Ocean Research and Development Activity
      NSTL Station
      Bay St. Louis, MS 39522

12.   LT B.B. Stamey, Jr.   4
      5508 Buskirk Street
      North Charleston, SC 29406